Planet. Space Sci., Vol. 36, No. 12, pp. 1391–1414, 1988
Printed in Great Britain.

0032–0633/88 $3.00 + 0.00
Pergamon Press plc

OZONE, CLIMATE AND BIOSPHERIC ENVIRONMENT IN THE ANCIENT OXYGEN-POOR ATMOSPHERE

L. M. FRANÇOIS and J.-C. GÉRARD
Institut d'Astrophysique, Université de Liège, B-4200 Ougrée-Liège, Belgium

(*Received in final form* 8 *July* 1988)

Abstract—To study the climatological role of ozone in the Precambrian atmosphere and the consequences of its reduction for the ultraviolet environment of the early biosphere, a coupled one-dimensional radiative–convective and photochemical model has been developed. Oxygen levels between 10^{-5} and 1 time the present atmospheric level (PAL) are considered. It is shown that when the ice–albedo feedback is taken into account, relatively important temperature decreases are associated with the ozone changes linked to the progressive decrease of the oxygen level from 1 PAL to smaller values.

A similar study is performed for enhanced atmospheric CO_2 pressures (P_{CO_2}). In these conditions, the ozone column is increased at low O_2 concentrations with respect to the $P_{CO_2} = 1$ PAL case. Consequently, the larger CO_2 concentration in the ancient atmosphere could have contributed to strengthen the ultraviolet screening of ozone. The surface temperature response to the ozone decrease, as well as the thermal profiles are also analyzed in these CO_2-rich models. A possible evolutionary scenario of atmospheric O_2 and CO_2 is discussed.

The consequences of these calculations for the ultraviolet environment of the primitive biosphere is discussed with a quantitative model calculating bacterial surviving rates. According to this model, the minimum ozone column being tolerable by unprotected bacteria would fall between $\sim 1 \times 10^{18}$ and $\sim 4 \times 10^{18}$ cm^{-2}, depending on the bacterial species considered and corresponding to an O_2 level somewhat lower than 10^{-2} PAL. For the coccoid blue–green alga *Agmenellum quadruplicatum*, this minimum ozone column would be of $\sim 4.5 \times 10^{18}$, a value which is only slightly less than the presently observed column in the spring time ozone hole of Antarctica.

1. INTRODUCTION

Geological evidences clearly demonstrate (Holland, 1984; Walker, 1977) that the ancient atmosphere of the Earth was much poorer in oxygen than today. It is difficult to describe quantitatively the evolution of atmospheric oxygen. Some broad limits are imposed by biological and geological constraints for various periods of the Earth's history, but even the interpretation of these indicators is still much debated today (Kasting, 1987, and references therein). The photochemistry of the troposphere and stratosphere was largely affected by the gradual release of oxygen into the atmosphere by photosynthesis. In particular, the shape of the ozone profile was continuously modified, as oxygen accumulated in the atmosphere. In the past, many studies were devoted to this problem. Berkner and Marshall (1965) were the first to consider the relationship between ozone and oxygen, they discussed with some details the biological effects of lower O_2 and O_3 amounts and proposed a general time-evolution of atmospheric oxygen. Ratner and Walker (1972) developed a simple model involving the basic chemistry of O and O_3 to calculate the ozone profiles at photochemical equilibrium. Afterwards, more precise calculations were performed with the addition of the chemistry of HO_x (Hesstvedt *et al.*, 1974) and NO_x (Blake and Carver, 1977). The effects of vertical transport, as well as the chemistry of N_2O were introduced by Levine *et al.* (1979) and Kasting and Donahue (1980). The latter group also added the implicit calculation of the O_2 profile and the oxidation chain of methane. Levine *et al.* (1981) made a further improvement by taking the chlorine chemistry into account. Finally, Kasting *et al.* (1985) have included the effect of Rayleigh scattering in a model that they used to study the oxidative power of H_2O_2.

The climatic role of ozone at reduced O_2 amounts is also an interesting field of research. However, there exists no complete study of this subject in the literature and, moreover, the existing models cannot be easily compared, in view of the different assumptions made for the calculation. In addition, very few calculations considered the coupling between temperature and photochemistry. Morss and Kuhn (1978) derived the temperature profiles for prescribed atmospheric compositions at various epochs in the Earth's history. Probably the most interesting works dealing with the climatic role of ozone in the ancient atmosphere are the coupled radiative–convective–photochemical

models of Levine and Boughner (1979) and Visconti (1982). The first group calculated the temperature profile at 10^{-1} PAL of O_2. Their photochemical scheme was taken from Levine *et al.* (1979). The other author made a similar calculation for 10^{-3} PAL of O_2 and for various amounts of CO_2 and CH_4. However, the ozone profiles that he derived show important discrepancies with the results of Kasting and Donahue (1980) and Levine *et al.* (1981). Indeed, in Visconti's calculations, the ozone maximum is located at ground level and only a small inflexion is present between 10 and 20 km.

Recently, the problem of the climatological role of O_3 in oxygen-poor atmospheres has acquired a new interest. Indeed, Williams and Sonnet (1985) found a clear solar signal (connected with the 11 y sunspot cycle) in the thicknesses of a series of Precambriam varves in the Elatina Formation of South Australia. Varve formation is related to fluctuations in surface climate and runoff conditions. Thus, the solar signature in the Elatina varves possibly testifies to the existence of an ancient solar control of climate with an 11 y periodicity. At present, the mechanism linking the climate to the solar variability is not known. However, the concentration of atmospheric ozone has varied with an 11 y periodicity, due to the variability in the solar ultraviolet spectrum. These ozone fluctuations possibly modulated the surface climate with the same periodicity (Gérard and François, 1987), since when the atmospheric oxygen was less abundant, the mean altitude of the ozone layer was lower.

Thus, it is of interest to re-examine the climatic role of ozone in the paleoatmosphere. Such an analysis is proposed in this paper, as well as an extension of the photochemical model to larger amounts of CO_2. Indeed, the ozone column density is dependent on the atmospheric mixing ratios of CO_2, so that it is important to test the sensitivity of the model to the presence of possibly large concentrations of this gas. Further, in this study, the vertical temperature profiles in a CO_2-rich atmosphere containing 10^{-5} to 10^{-2} PAL of O_2 are compared with those calculated for 1 PAL of CO_2. The time evolution of carbon dioxide proposed by Hart (1978) is used together with a likely history of atmospheric oxygen to derive a possible evolutionary scenario for the Earth's global mean surface temperature. The results of this calculation clearly show that the role of oxygen and ozone is not negligible in determining the climatological history of the Earth. Finally, in the last section, we present an analysis of the effects on the early biosphere of the enhanced ultraviolet radiation at the Earth's surface associated with the lower O_2 amounts in the paleoatmosphere.

2. MODEL

2.1. *Photochemistry*

The altitude distribution of the atmospheric species is calculated using a one-dimensional photochemical model. The continuity and flux equations are solved for $O_x(O, O_3)$, O_2, H, OH, HO_2, H_2O_2, H_2, CO, CO_2, CH_4, CH_3COOH, N_2O, $NO_x(NO, NO_2)$, N_2O_5, HNO_2 and HNO_3. The distribution of water vapour is fixed consistently with the temperature profile in the radiative–convective calculation. The following species are assumed in photochemical equilibrium at each altitude: $O(^1D)$, $N(^4S)$, $^1CH_2$, $^3CH_2$, CH_3, CH_3O_2, HCO, H_2CO, H_3CO, NO_3 and N_2O_4.

The O_2 level refers to the oxygen mixing ratio f_{O_2} at the ground, which is fixed in each model. Six different levels are considered, from 10^{-5} to 1 PAL (present atmospheric level). For $[O_2] = 10^{-1}$ and 1 PAL, the oxygen mixing ratio is kept constant at each height in the atmosphere. By contrast, for $[O_2] \leqslant 10^{-2}$ PAL, the oxygen profile is internally calculated, since it may somewhat depart from hydrostatic equilibrium for the lowest O_2 levels.

The model extends from the ground to 70 km in steps of 1 km. It includes 106 chemical reactions, of which 23 are photodissociation processes (Table 1). For the calculation of the photolysis rates, a solar zenith angle of 60° is assumed and a 0.5 multiplying factor is included to account for the day–night alternation. The solar irradiances reported by Brasseur and Simon (1981) are adopted. The eddy diffusion profile is taken from Hunten (1975). Rainout from the troposphere is considered for HNO_3, HNO_2, N_2O_5, N_2O_4, H_2O_2, CH_3OOH and H_2CO, using the method of Fishman and Crutzen (1977). Following Kasting and Donahue (1980), the vertical distribution of nitrous oxide is calculated by assuming a modern upward flux at the ground. The methane mixing ratio at ground level is fixed to the modern value of 1.6 ppmv.

The surface pressure is $P_0 = 1$ atm at $[O_2] = 1$ PAL, $P_0 = 0.81$ atm at $[O_2] = 10^{-1}$ PAL and $P_0 = 0.79$ atm for lower O_2 levels. The vertical profiles of pressure and total concentration are calculated consistently with temperature, composition and surface pressure.

2.2. *Radiative–convective model*

For the radiative–convective calculation, the model of Gérard and François (1988) has been used. A short description will be given here. The atmosphere is divided into 26 layers equally spaced in log-pressure coordinates, from P_0 at the ground to $4 \times 10^{-5}\ P_0$ at the top of the model. The altitude of each layer is calculated from the knowledge of the atmospheric

TABLE 1. REACTIONS AND RATE CONSTANTS

Reaction	Rate constant ($cm^3\ s^{-1}$ or $cm^6\ s^{-1}$)	Reference
(1) $O_2+h\nu \rightarrow O+O$	J_{O_2}	JPL 85
(2) $O_2+h\nu \rightarrow O+O(^1D)$	J_{O_2}	JPL 85
(3) $O_3+h\nu \rightarrow O_2+O$	J_{O_3}	JPL 85
(4) $O_3+h\nu \rightarrow O_2+O(^1D)$	J_{O_3}	JPL 85
(5) $O+O_2+M \rightarrow O_3+M$	$6\times10^{-34}(T/300)^{-2.3}$	JPL 85
(6) $O+O+M \rightarrow O_2+M$	$2.76\times10^{-34}\exp(710/T)$	Campbell and Thrush (1967)
(7) $O+O_3 \rightarrow O_2+O_2$	$8\times10^{-12}\exp(-2060/T)$	JPL 85
(8) $O+H_2 \rightarrow OH+H$	$3\times10^{-14}\exp(-4480/T)$	Hampson and Garvin (1977)
(9) $O(^1D)+N_2 \rightarrow O+N_2$	$1.8\times10^{-11}\exp(107/T)$	JPL 85
(10) $O(^1D)+O_2 \rightarrow O+O_2$	$3.2\times10^{-11}\exp(67/T)$	JPL 85
(11) $O(^1D)+H_2 \rightarrow OH+H$	1×10^{-10}	JPL 85
(12) $O(^1D)+H_2O \rightarrow OH+OH$	2.2×10^{-10}	JPL 85
(13) $H_2O+h\nu \rightarrow OH+H$	J_{H_2O}	Thompson *et al.* (1963)
(14) $HO_2+h\nu \rightarrow OH+O$	J_{HO_2}	JPL 85
(15) $H_2O_2+h\nu \rightarrow OH+OH$	$J_{H_2O_2}$	JPL 85
(16) $H+O_2+M \rightarrow HO_2+M$	three body rate	JPL 85
(17) $H+O_3 \rightarrow OH+O_2$	$1.4\times10^{-10}\exp(-470/T)$	JPL 85
(18) $H+H+M \rightarrow H_2+M$	$2.6\times10^{-33}\exp(-375/T)$	Liu and Donahue (1974)
(19) $H+OH+M \rightarrow H_2O+M$	$6.1\times10^{-26}/T^2$	McEwan and Phillips (1975)
(20) $H+HO_2 \rightarrow H_2+O_2$	$0.09\times7.4\times10^{-11}$	JPL 85
(21) $H+HO_2 \rightarrow H_2O+O$	$0.04\times7.4\times10^{-11}$	JPL 85
(22) $H+HO_2 \rightarrow OH+OH$	$0.87\times7.4\times10^{-11}$	JPL 85
(23) $OH+O \rightarrow O_2+H$	$2.2\times10^{-11}\exp(117/T)$	JPL 85
(24) $OH+O_3 \rightarrow HO_2+O_2$	$1.6\times10^{-12}\exp(-940/T)$	JPL 85
(25) $OH+HO_2 \rightarrow H_2O+O_2$	$1.7\times10^{-11}\exp(416/T)$ $+3\times10^{-31}[M]\exp(500/T)$	JPL 85
(26) $OH+H_2 \rightarrow H_2O+H$	$6.1\times10^{12}\exp(-2030/T)$	JPL 85
(27) $OH+OH \rightarrow H_2O+O$	$4.6\times10^{-12}\exp(-242/T)$	JPL 85
(28) $OH+OH+M \rightarrow H_2O_2+M$	three body rate†	JPL 85
(29) $HO_2+HO_2 \rightarrow H_2O_2+O_2$	$2.3\times10^{-13}\exp(590/T)$ $+1.7\times10^{-33}[M]\exp(1000/T)$	JPL 85
(30) $HO_2+O \rightarrow OH+O_2$	$3\times10^{-11}\exp(200/T)$	JPL 85
(31) $HO_2+O_3 \rightarrow OH+2O_2$	$1.4\times10^{-14}\exp(-580/T)$	JPL 85
(32) $H_2O_2+OH \rightarrow H_2O+HO_2$	$3.1\times10^{-12}\exp(-187/T)$	JPL 85
(33) $N_2O+h\nu \rightarrow N_2+O$	J_{N_2O}	(*)
(34) $N_2O+h\nu \rightarrow N_2+O(^1D)$	J_{N_2O}	(*)
(35) $N_2O+O(^1D) \rightarrow N_2+O_2$	4.9×10^{-11}	JPL 85
(36) $N_2O+O(^1D) \rightarrow NO+NO$	6.7×10^{-11}	JPL 85
(37) $N+O_2 \rightarrow NO+O$	$4.4\times10^{-12}\exp(-3220/T)$	JPL 85
(38) $N+NO \rightarrow N_2+O$	3.4×10^{-11}	JPL 85
(39) $N+NO_2 \rightarrow N_2O+O$	3×10^{-12}	JPL 85
(40) $NO+h\nu \rightarrow N+O$	J_{NO}	Brasseur and Solomon (1984)
(41) $NO+HO_2 \rightarrow NO_2+OH$	$3.7\times10^{-12}\exp(5240)/T)$	JPL 85
(42) $NO+O_3 \rightarrow NO_2+O_2$	$1.8\times10^{-12}\exp(1370/T)$	JPL 85
(43) $NO+OH+M \rightarrow HNO_2+M$	three body rate	JPL 85
(44) $NO+NO+O_2 \rightarrow 2NO_2+M$	$3.3\times10^{-39}\exp(350/T)$	Report FAA-EE-80 (1980)
(45) $NO_2+h\nu \rightarrow 2NO+O$	J_{NO_2}	JPL 85
(46) $NO_2+H \rightarrow OH+NO$	$4.8\times10^{-10}\exp(-400/T)$	Clyne and Monkhouse (1977)
(47) $NO_2+O \rightarrow NO+O_2$	9.3×10^{-12}	JPL 85
(48) $NO_2+O_3 \rightarrow NO_3+O_2$	$1.2\times10^{-13}\exp(-2450/T)$	JPL 85
(49) $NO_2+OH+M \rightarrow HNO_3+O_2$	three body rate	JPL 85
(50) $NO_2+NO+H_2O \rightarrow 2HNO_2+O_2$	6×10^{-38}	Report FAA-EE-80 (1980)
(51) $NO_2+NO+O_2 \rightarrow NO_3+NO_2$	$2\times10^{-41}\exp(400/T)$	Report FAA-EE-80 (1980)
(52) $NO_2+NO_2+M \rightarrow N_2O_4+M$	$3\times10^{-35}\exp(1040/T)$	Report FAA-EE-80 (1980)
(53) $NO_3+h\nu \rightarrow NO+O_2$	J_{NO_3}	JPL 85
(54) $NO_3+h\nu \rightarrow NO_2+O$	J_{NO_3}	JPL 85
(55) $NO_3+NO \rightarrow 2NO_2$	$1.3\times10^{-11}\exp(250/T)$	JPL 85
(56) $NO_3+NO_2 \rightarrow NO+NO_2+O_2$	$2.3\times10^{-13}\exp(-1000/T)$	Hampson and Garvin (1977)
(57) $NO_3+NO_2+M \rightarrow N_2O_5+M$	three body rate	Hampson and Garvin (1977)
(58) $N_2O_4+M \rightarrow NO_2+NO_2+M$	$4.2\times10^{-7}\exp(-1000T)$	JPL 85
(59) $N_2O_5+h\nu \rightarrow NO_3+NO_2$	$J_{N_2O_5}$	JPL 85

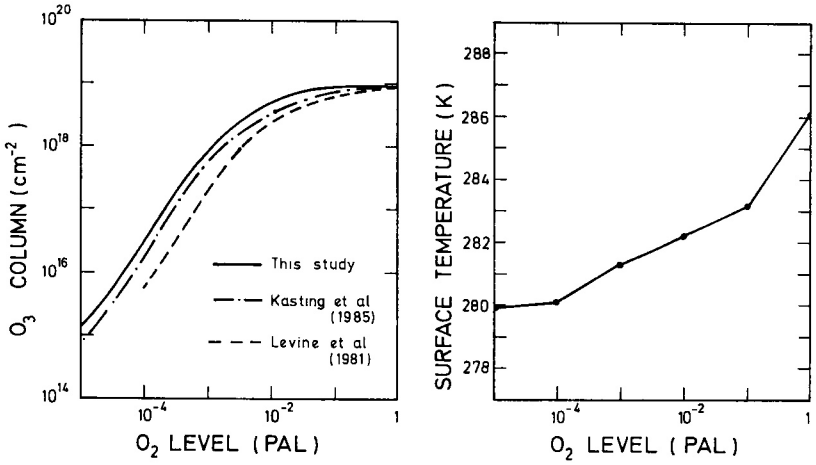

FIG. 1. OZONE COLUMN DENSITY AND GLOBAL MEAN SURFACE TEMPERATURE AS A FUNCTION OF THE OXYGEN LEVEL EXPRESSED IN PAL (PRESENT ATMOSPHERIC LEVEL).
The results for the ozone column are compared with those of previous studies.

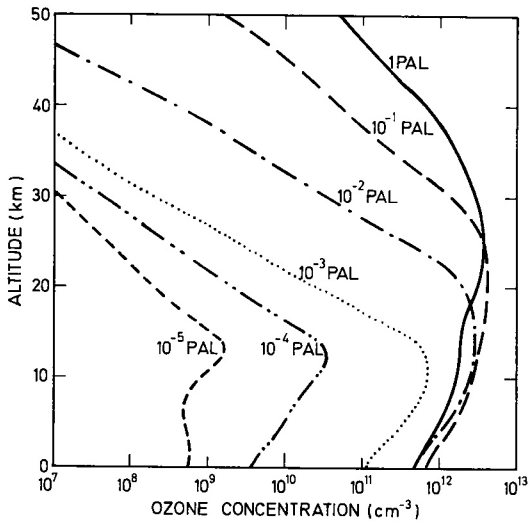

FIG. 2. VERTICAL PROFILES OF THE OZONE CONCENTRATION FOR O_2 LEVELS VARYING FROM 10^{-5} TO 1 PAL.

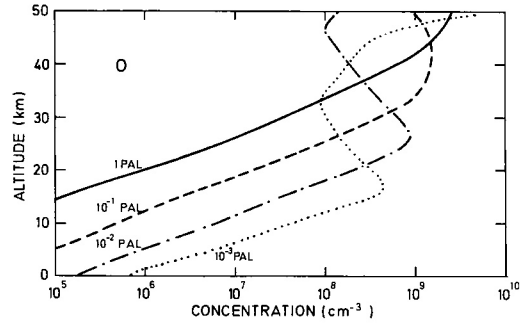

FIG. 3. VERTICAL PROFILES OF ATOMIC OXYGEN FOR 10^{-3}, 10^{-2}, 10^{-1} AND 1 PAL OF O_2.

that presented by Kasting (1979). In our model, the OH and HO_2 abundances are not very dependent on the oxygen level, at least for the O_2 levels considered in Fig. 4. The concentration of the hydroxyl radical is progressively increased, as O_2 is removed from the atmosphere. However, this increase is much less pronounced than in the model of Levine *et al.* (1981). For example, in our model, the ground level concentration of OH is changed from 9.5×10^5 to 6.6×10^6 cm^{-3}, when the O_2 level is varied from 1 to 10^{-5} PAL, which is much smaller than the ~ 1000 fold increase between 1 and 10^{-4} PAL predicted by Levine *et al.* (1981), but compares well with the results of Kasting *et al.* (1985). The HO_2 concentration at ground level is still much less variable, since it almost does not change between 1 and 10^{-2} PAL and is increased by only a factor of ~ 2 at lower O_2 levels. Again, this behaviour is in very good agreement with the calculation of Kasting *et al.* (1985). By contrast, the NO and NO_2 profiles shows a sharp dependence on the O_2 abundance. This is linked to the calculation of the N_2O profile. Indeed, following Kasting and Donahue (1980), it is assumed that the upward flux of nitrous oxide at the ground (simulating the biological production) is constant and equal to 1.89×10^9 cm^2 s^{-1}, independently of the O_2 level. With this assumption, the concentration of nitrous oxide is much smaller in an oxygen-poor atmosphere, when compared with present conditions, owing to the larger rate of N_2O

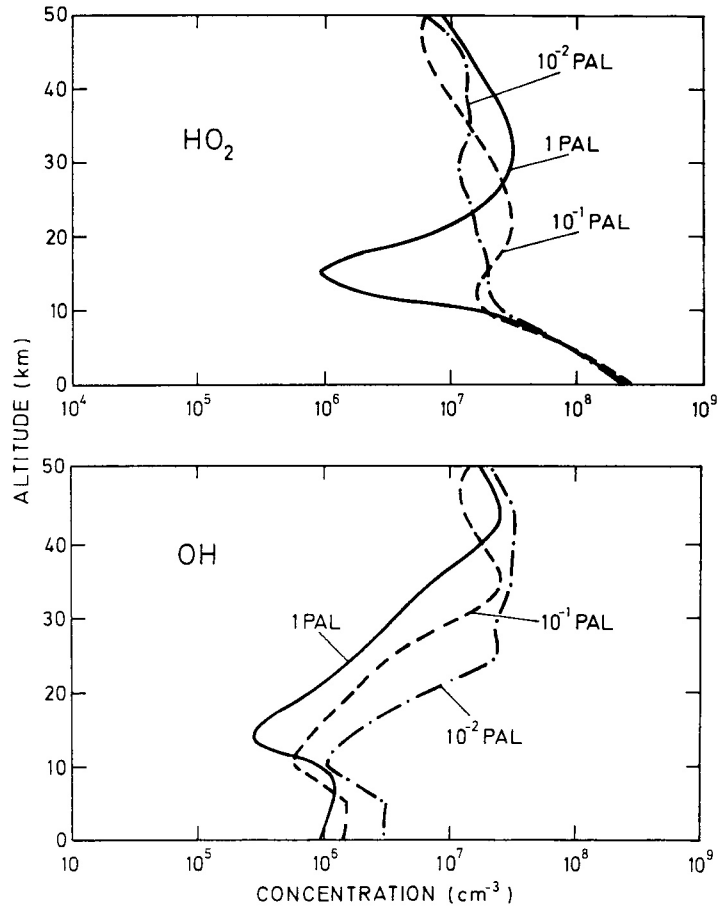

FIG. 4. VERTICAL PROFILES OF HO_2 AND OH FOR 10^{-2}, 10^{-1} AND 1 PAL OF O_2.

photolysis. It follows that the mixing ratios of the NO_x species are strongly decreased and that their effects on the ozone chemistry are reduced.

The main purpose of this section is the study of the climatological changes linked to the decrease of atmospheric oxygen and ozone. This problem was partially studied earlier by Levine and Boughner (1979), who calculated the vertical temperature profile at 10^{-1} PAL of O_2 and compared it with the 1 PAL case. They assumed a constant 6.5 K km^{-1} lapse rate in the convective region and a fixed reflectivity of the Earth's surface. A similar calculation is performed here for O_2 levels varying from 10^{-5} to 1 PAL. As mentioned in the model description, we use a moist adiabatic lapse rate and a varying surface albedo, which are probably more realistic assumptions than those adopted by Levine and Boughner (1979). The right-hand part of Fig. 1 shows the evolution of the surface temperature T_s as the atmospheric oxygen level is increased. For $[O_2] = 1$ PAL, $T_s = 286.15$ K, not far from the present global mean value of the Earth's surface temperature.

When f_{O_2} is reduced from 1 to 10^{-1} PAL, the resulting temperature change is due to several competing effects, as shown by the analysis of Levine and Boughner (1979). In their model, the oxygen decrease generates a substantial increase of the ozone column (+30%) and the altitude of the peak concentration is moved downwards. The total effect of this redistribution and column increase of ozone is to warm the surface by 4.5 K. This warming is the consequence of an increased greenhouse effect of O_3, a decrease in the visible albedo due to the larger O_3 column, and greenhouse and albedo variations linked to changes in H_2O concentration. On the other side, the reduction of total pressure associated with the lower abundance of atmospheric oxygen creates a 5 K decrease of the surface temperature, as a result of reduced line broad-

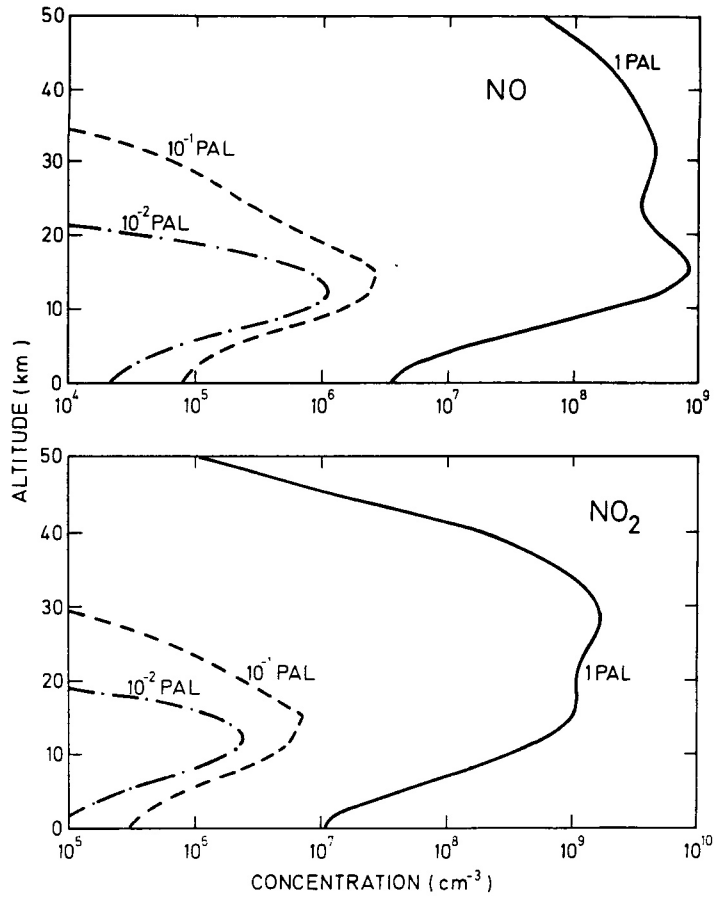

FIG. 5. VERTICAL PROFILES OF NO AND NO_2 for 10^{-2}, 10^{-1} AND 1 PAL OF O_2.

ening on the H_2O and CO_2 infrared bands and the reduced H_2O and CO_2 amounts. Thus, the model of Levine and Boughner produces only a small net cooling of 0.5 K when the O_2 level is changed from 1 to 10^{-1} PAL and the total pressure is reduced accordingly.

As shown in Fig. 1, the present model predicts a 3.0 K decrease of the surface temperature in the same conditions (lower total pressure and $f_{O_2} = 10^{-1}$ PAL). This larger cooling may be attributed in part to the much smaller increase (2%) of the ozone column density in our model. If the mixing ratio of oxygen is decreased from 1 to 10^{-1} PAL without any change in the total pressure, the surface temperature remains almost constant ($\Delta T_s = +0.08$ K). Thus, the temperature difference between the 1 and 10^{-1} PAL models in our calculation is due mainly to the reduction of the surface pressure, but the amplitude of the associated cooling is smaller by ~ 2 K with respect to the results of Levine and Boughner (1979). We attribute this lower sensitivity to the use of a moist adiabatic lapse rate in our convective code. Indeed, the use of such an adiabatic lapse rate may decrease the sensitivity of a radiative–convective model by a significant factor (Lindzen *et al.*, 1982; Gérard and François, 1988), with respect to the case where it is fixed to 6.5 K km^{-1} as in the calculation of Levine and Boughner (1979).

A further decrease of the O_2 level to 10^{-2} PAL ($P_0 = 0.79$ atm) does not cool the surface but warms it by 0.05 K, with respect to the 10^{-1} PAL ($P_0 = 0.81$ atm) case, despite the associated 45% decrease of the total ozone column. The small warming is due to the larger relative change of ozone at high altitude compared with lower in the atmosphere (see Fig. 2). Indeed, decreasing the concentration of high altitude ozone tends to warm the surface as a result of a less important stratospheric absorption of solar radiation, while a similar change at low altitude cools the surface due to the reduced greenhouse warming (Ramanathan

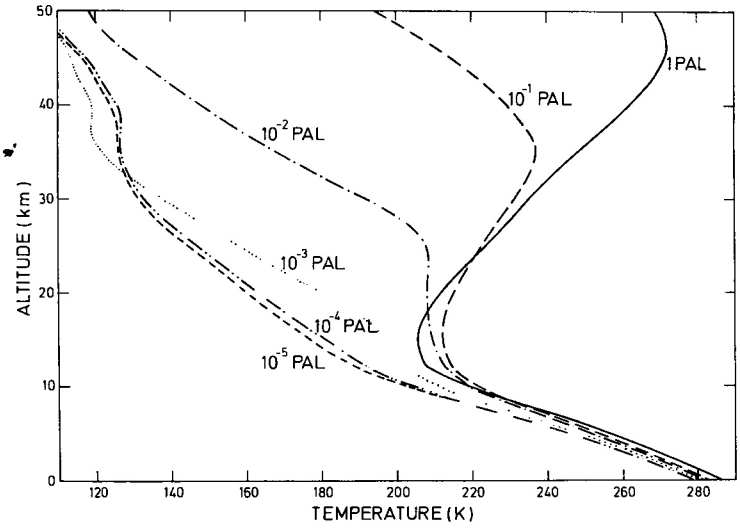

FIG. 6. VERTICAL TEMPERATURE PROFILES FOR OXYGEN LEVELS VARYING FROM 10^{-5} TO 1 PAL.

and Dickinson, 1979; Wang *et al.*, 1980; François, 1988). A still larger reduction of the ozone column is observed when f_{O_2} is decreased from 10^{-2} to 10^{-3} PAL. In this case, the variation of the ozone concentration takes place closer to the ground and a strong cooling is obtained ($\Delta T_s = 1.8$ K). Between 10^{-3} and 10^{-4} PAL, the ozone density becomes small, but the surface temperature change remains important ($\Delta T_s = 1.2$ K). This result is due to the large ozone reduction in the 10–20 km region between 10^{-3} and 10^{-4} PAL. Indeed, the work of Wang *et al.* (1980), confirmed by a more recent study by François (1988), shows that the sensitivity of the surface climate maximizes when the ozone perturbations are located in this altitude range (the 10–20 km region is the most effective for the greenhouse warming of ozone). Between 10^{-4} and 10^{-5} PAL, the surface is cooled by only 0.2 K, due to the smaller change of the ozone column between these O_2 levels. Note, however, that ozone still plays a climatic role at 10^{-5} PAL of oxygen, since, when all the ozone is removed from this 10^{-5} PAL atmosphere, the surface temperature is further decreased by 1 K. Consequently, if all oxygen and ozone were removed from the present atmosphere, a global decrease of 7.2 K of the mean surface temperature of the Earth is predicted. This value accounts for the change in the greenhouse effect of ozone, but also for the variations in the distribution of water vapour and for the decrease in total pressure. It may be compared with the slightly smaller (5 K) value obtained by Kasting (1987) in the same conditions.

In Fig. 6, the vertical temperature profiles calculated with our model are presented for O_2 varying from 10^{-5} to 1 PAL. These profiles show the progressive development of the stratosphere, as the oxygen abundance is increased. Although there are major variations in the stratospheric temperature profile, the top of the convective region is located in each case in the same altitude range (10–14 km). The temperature profile at 10^{-1} PAL of O_2 is in fairly good agreement with the calculation of Levine *et al.* (1980). A small stratospheric maximum is observed between 30 and 40 km and the tropopause minimum is slightly higher and warmer than today. In the upper stratosphere, the temperature is lowered with respect to the 1 PAL case, owing to the smaller ozone concentration in this region. This situation is reversed in the lower stratosphere, where the ozone concentration is increased. A similar behaviour is observed for the thermal structure at 10^{-2} PAL: between 10 and 18 km, the temperature is slightly larger than for 1 PAL of O_2. However, in this latter case, the upper stratospheric ozone is not abundant enough to produce a temperature maximum in this region. Consequently, the temperature decreases with altitude in the whole stratosphere and is as low as 120 K and 50 km. For $f_{O_2} = 10^{-3}$ PAL, the only effect of O_3 (in addition to its greenhouse effect tending to warm the surface) is to create a small curvature in the thermal profile. Finally, at 10^{-4} and 10^{-5} PAL, ozone seems to become negligible in shaping the thermal profile, so that a regular temperature decrease is observed throughout the atmosphere.

To analyze the effects of coupling the calculations of photochemistry and temperature, we have run a further model at 10^{-4} PAL of O_2, in which the thermal

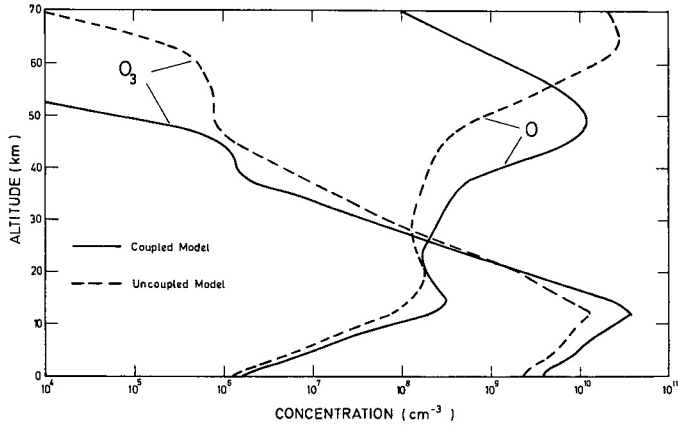

FIG. 7. COMPARISON OF THE OZONE AND ATOMIC OXYGEN PROFILES OBTAINED BY COUPLING THE CALCULATIONS OF PHOTOCHEMISTRY AND THERMAL STRUCTURE (FULL LINE) OR BY USING THE PHOTOCHEMICAL SCHEME ALONE WITH A FIXED TEMPERATURE PROFILE (DASHED LINE).
The oxygen level is 10^{-4} PAL.

structure was held fixed. In the troposphere, we used the temperature profile calculated for 1 PAL of O_2 (i.e. a profile with a too large T_s value), whereas, in the stratosphere, following Kasting (1979) and Kasting and Donahue (1980), we let the temperature decrease linearly between the tropopause and the mesopause. Similarly, in the lower atmosphere, the 1 PAL water vapour profile was used, in accordance with the adopted temperature structure in this region, whereas, above 15 km, the H_2O mixing ratio was fixed to that of the coupled 10^{-4} PAL model. This uncoupled calculation yields an ozone column density of $\sim 1.1 \times 10^{16}$ cm^{-2}, that is less than 40% of that obtained with the coupled scheme. This value is somewhat lower than that derived by Kasting *et al.* (1985), indicating that the difference between their and our results (see Fig. 1) is at least partly due to the different temperature profiles. In Fig. 7, the atomic oxygen and ozone profiles calculated with the coupled and uncoupled models have been plotted. As is obvious in this figure, the lower total ozone column in the uncoupled scheme arises from a lower ozone density in the whole troposphere. This observation may be explained by the larger abundance of HO_x in this region, as a result of wetter conditions associated with the larger tropospheric temperature. For the same reason, the atomic oxygen density is also reduced throughout the troposphere. Above 20 km, the model behaviour is reversed: the concentrations of atomic oxygen and ozone are higher in the uncoupled calculation. As previously mentioned, the mixing ratio of water vapour is the same in both models, above 15 km. Thus, the difference between the two calculations in the upper atmosphere may not be attributed to

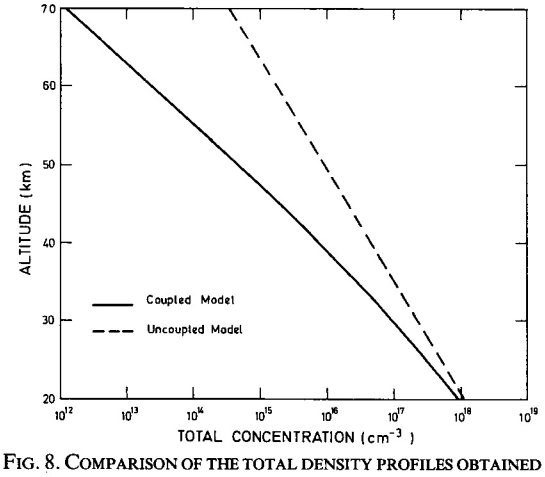

FIG. 8. COMPARISON OF THE TOTAL DENSITY PROFILES OBTAINED BY COUPLING THE CALCULATIONS OF PHOTOCHEMISTRY AND THERMAL STRUCTURE (FULL LINE) OR BY USING THE PHOTOCHEMICAL SCHEME ALONE WITH A FIXED TEMPERATURE PROFILE (DASHED LINE).
The oxygen level is 10^{-4} PAL.

H_2O, but another temperature effect must be searched for. Actually, as shown in Fig. 8, the difference is due to the lower total density in the coupled model. Indeed, the lower stratospheric temperature in this model results in a smaller scale height throughout the stratosphere, producing a lower total density in the upper atmosphere. As shown in Fig. 9, this reduction in the total density enables a deeper penetration of the radiation photodissociating O_2. For example, the radiation with wavelength near 150 nm is absorbed at an altitude $\sim$20 km lower in the coupled scheme. It is the reason why, in Fig. 7, the stratospheric peak of

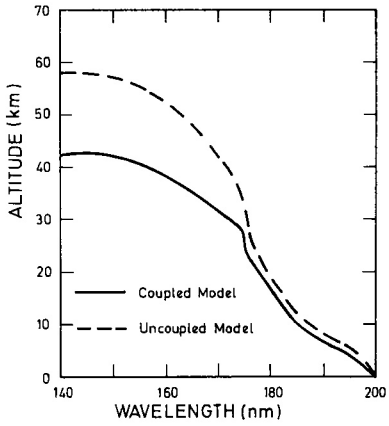

FIG. 9. ALTITUDES OF UNIT OPTICAL DEPTH FOR THE RADIATION BELOW 200 nm CALCULATED BY CONSIDERING THE COUPLING BETWEEN PHOTOCHEMISTRY AND THERMAL STRUCTURE (FULL LINE) OR BY USING THE PHOTOCHEMICAL SCHEME ALONE WITH A FIXED TEMPERATURE PROFILE (DASHED LINE).
The oxygen level is 10^{-4} PAL.

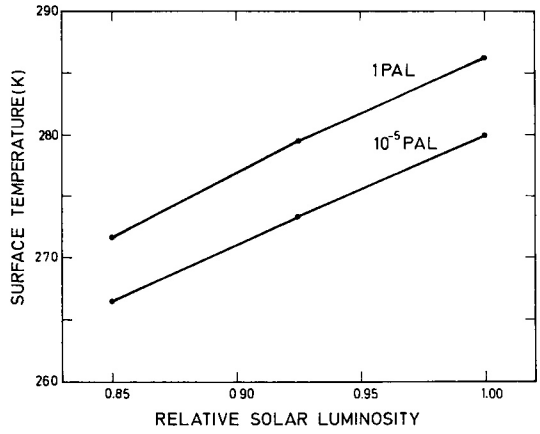

FIG. 10. GLOBAL MEAN SURFACE TEMPERATURE AS A FUNCTION OF THE RELATIVE SOLAR LUMINOSITY $L/L_{\odot}$.
Two curves are displayed, one for 10^{-5} and the other for 1 PAL of O_2

atomic oxygen, as well as the small kink in the ozone profile, are shifted ~20 km downward, when the temperature is calculated consistently with photochemistry. Thus, in conclusion, our model predicts two major effects arising from coupling the calculations of temperature and chemistry, depending on the atmospheric region taken into consideration. In the troposphere, the lower temperature in the coupled scheme increases the O_x density, through the reduction of the water (and thus HO_x) partial pressure. In the upper atmosphere, the total density is decreased and the depth of penetration of the radiation with wavelength falling short of 200 nm is lowered, producing a global downward shift of the O and O_3 profiles.

In the past, the solar luminosity was lower than today. In this context, it is of interest to estimate the climatic effects of ozone at reduced solar luminosities. Indeed, several theoretical studies have been devoted to the problem of the low luminosity of the early Sun (Sagan and Mullen, 1972; Kasting *et al.*, 1984; Kiehl and Dickinson, 1987). The present work shows that the removal of oxygen and ozone from the modern atmosphere can generate a substantial surface temperature decrease (7.2 K). Since such a cooling is not negligible, it is important to take it into account in climatic studies of the ancient atmosphere. Thus, our radiative–convective model has been run for reduced solar luminosities with the ozone profiles given in Fig. 2 for 1 and 10^{-5} PAL (with $P_0 = 1$ and 0.79 atm respectively). The results for the surface temperature are displayed in Fig. 10. The surface temperature change between 1 and 10^{-5} PAL is 6.2 K for present solar conditions, while it is only 5.1 K for a relative solar luminosity $L/L_{\odot} = 0.85$. In the latter case, the mean surface temperature is lower. With such a cold climate, the ice–albedo feedback is more efficient. This effect should enhance the climate sensitivity. However, under such conditions, the troposphere is much dryer and the climatic feedback of water vapour is reduced. Since the temperature change associated with the decrease of oxygen from 1 to 10^{-5} PAL is lower for $L/L_{\odot} = 0.85$, it appears that the second mechanism is prevailing. This conclusion depends, however, on the adopted parameterization for the ice–albedo feedback. Nevertheless, the present calculation shows that the lower abundance of oxygen and ozone may be important in describing ancient climates with numerical models.

4. THE ROLE OF AN ENHANCED CO_2 LEVEL

During the Precambrian, the atmospheric level of carbon dioxide was substantially larger than today. This increased amount of CO_2 was mainly suggested as a compensation for the reduced luminosity of the early Sun. Indeed, to explain the lack of evidence of global glaciations in the geological record, it is necessary to postulate the existence of a greenhouse gas in the atmosphere at the time when the solar luminosity was lower. Among the possible atmospheric greenhouse gases, CO_2 appears to be the most likely, since the rate of release of the other candidates was presumably too small to account for the large warming required. Further, Walker *et al.* (1981) proposed a feedback mechanism linking the carbon dioxide pressure P_{CO_2} and the mean surface temperature T_s. This

process stabilizes the Earth's climate by decreasing the CO_2 geochemical sink associated with silicate weathering, so that a decrease in T_s tends to be damped by a simultaneous increase of P_{CO_2}.

Since the solar luminosity has increased almost linearly from the early Precambrian until now (e.g. Endal and Schatten, 1982), the concentration of atmospheric CO_2 must become progressively larger as we go further back into the past. Hart (1978) has derived the history of ancient CO_2 from a simple geochemical model. In view of the numerous unknowns linked to the problem of the atmospheric evolution, the results of this model must be considered as highly speculative. Nevertheless, this CO_2 scenario has been tested with radiative–convective calculations by several authors (Owen *et al.*, 1979; Kasting *et al.*, 1984; Kiehl and Dickinson, 1987). These studies show that Hart's CO_2 scenario is approximately thermostatic. It appears that, during the early history of Earth, the minimum CO_2 level necessary to compensate for the reduced solar luminosity was several hundred times larger than its present atmospheric level. This conclusion was also confirmed by Kasting (1985), who calculated that 80 to 600 PAL of CO_2 must have been present in the early atmosphere when the solar luminosity was 25% lower than today, to maintain the mean surface temperature between 0 and 15°C. In the more recent past, after the release of oxygen by photosynthetic activity (the time period we are concerned with), the minimum CO_2 level was in the range of several to ~ 100 PAL. In Hart's evolutionary sequence, $P_{CO_2} = 103$ PAL 3 By ago, 27 PAL 2 By ago and 2 PAL 1 By ago.

In view of these larger CO_2 abundances in the past, it is of interest to test the sensitivity to the CO_2 pressure of the climatic and photochemical results discussed in the preceding section. For this calculation, we shall assume a CO_2 level of 100 PAL. According to Hart's scenario this value corresponds approximately to the time of the beginning of the photosynthetic activity. Thus, this high CO_2 level is probably only compatible with low oxygen abundances (10^{-5} PAL or below to possibly 10^{-3} PAL). Nevertheless, to make the comparison between the results easier, we shall adopt this value of P_{CO_2} for all the O_2 levels considered, postponing to the next section the description of a possible evolutionary scenario. Besides, the choice of a high CO_2 level will make the changes associated with the CO_2 increase more obvious.

At large P_{CO_2}, usual parameterizations of the longwave absorption by CO_2 are inappropriate. Narrow band models may be used, as in the calculation by Kiehl and Dickinson (1987). Here, as mentioned in the model section, we have preferred to adopt the parameterization developed by Kasting *et al.* (1984), for the CO_2 absorptance between 8.7 and 20.2 μm. This parameterization is based on laboratory measurements of CO_2 absorption by Burch *et al.* (1962). It may be used for pathlengths equivalent to a vertical path through an atmosphere containing 0.1 bar of CO_2. Thus, this method is entirely justified for the models with $P_{CO_2} = 100$ PAL.

The CO_2-rich model was run for oxygen levels varying from 10^{-5} to 10^{-2} PAL. To avoid the increase of the surface temperature to unrealistically high values, the solar luminosity was decreased by 15% with respect to its present value. The results for the ozone column and the surface temperature are displayed in Fig. 11, on the curves labeled $100 \times CO_2$. For comparison, the curves of Fig. 1 are reported on the same figure. The response of the total ozone column to the CO_2 increase depends on the amount of atmospheric oxygen considered. At low O_2 levels, the enhancement of CO_2 from 1 to 100 PAL generates a substantial increase of the ozone column. For example, at 10^{-5} PAL of O_2, an increase of about an order of magnitude is predicted. This effect may be of some importance for the habitability of the Precambrian Earth. This point will be examined in more detail in Section 6. By contrast, when the oxygen level is as high as 10^{-2} PAL, a small decrease (from 5×10^{18} to 3.7×10^{18} cm^{-2}) of the ozone column accompanies the CO_2 enhancement. The O_2 level where the behaviour of the system is reverted corresponds approximately to 10^{-3} PAL.

Before trying to explain this behaviour, we shall describe briefly the main features of the changes in the ozone profile, due to the CO_2 variation from 1 to 100 PAL. At 10^{-5} PAL of O_2, the ozone concentration is increased throughout the atmosphere by an approximately constant factor, except near the ground where this factor is somewhat smaller. This situation is quite similar at 10^{-4} PAL, except for the magnitude of the increase, which is significantly lower, as indicated by the much smaller change in the total column. At 10^{-3} PAL, low altitude ozone is no more affected by the CO_2 change, but just a slight increase is observed in the higher atmosphere, above the ozone peak. Since no change is present in the lower atmosphere where ozone is most abundant, the total column almost does not vary. At 10^{-2} PAL, the observed column decrease is due to a small reduction of the concentration in the vicinity of the ozone peak.

Such a behaviour may be understood by considering the changes in the O_x production at low altitude induced by the enhancement of carbon dioxide. Indeed, at low O_2 levels (10^{-5} PAL or below), the major source of O_x comes from photodissociation of carbon dioxide, while, at high O_2 levels, photo-

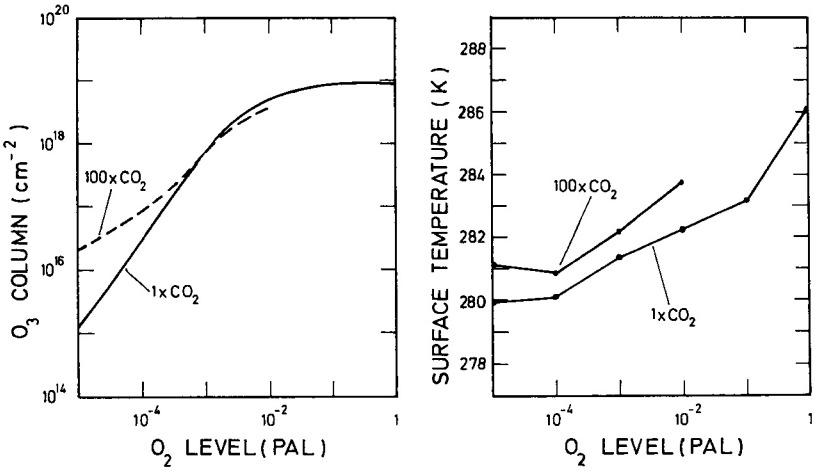

FIG. 11. OZONE COLUMN DENSITY AND GLOBAL MEAN SURFACE TEMPERATURE AS A FUNCTION OF THE OXYGEN LEVEL.
The results obtained in a CO_2-rich ($100 \times CO_2$) atmosphere are compared with those obtained under present amounts of this gas.

dissociation of O_2 becomes prevailing. The rate of CO_2 photodissociation naturally increases with CO_2, so that, for small mixing ratios of O_2, the O_x production increases with CO_2 a conclusion which explains the ozone increase with CO_2 observed in Fig. 11 for 10^{-5} and 10^{-4} PAL. By contrast, O_2 photodissociation is slightly slowed down by an increase of CO_2, due to the overlying absorptions of these gases. Thus, at 10^{-2} PAL of O_2, the O_x production is somewhat reduced when CO_2 is enhanced, corresponding to the small observed decrease of the ozone column. Nevertheless, this ozone reduction will always remain small, even for higher O_2 levels, since the relative magnitude of the CO_2 absorption decreases when the mixing ratio of O_2 becomes larger.

The steady-state mean surface temperature calculated for 100 PAL of CO_2 is also presented in Fig. 11 as a function of the oxygen level. The general shape of this curve is similar to that obtained at 1 PAL of CO_2, since the temperature decreases between 10^{-2} and 10^{-3} PAL and between 10^{-3} and 10^{-4} PAL are very close to the corresponding decreases calculated for 1 PAL of CO_2. However, in this CO_2-rich case, a warming of 0.36 K is observed when the oxygen level is varied from 10^{-4} to 10^{-5} PAL, instead of a cooling under CO_2-poor conditions. This result suggests that the solar radiation still plays a non negligible climatic role at these low O_2 levels, since it is the availability of more solar radiation at the ground that may warm the surface under reduced ozone concentrations. The temperature profiles for 100 PAL of CO_2 are shown in Fig. 12. The most important difference in the stratospheric thermal structure between the CO_2-poor (Fig. 1) and the CO_2-rich (Fig. 12) models is observed at 10^{-2} PAL of O_2 in the lower stratosphere. Indeed, in this case, the 12–25 km region is almost isothermal with a temperature of $\sim$208 K for 1 PAL of CO_2, whereas for 100 PAL, the temperature profile shows only a small curvature in this region, with temperature decreasing regularly to reach on the average a smaller value through the lower stratosphere. This average temperature decrease is due to the larger radiative cooling by CO_2 in the stratosphere. The other temperature profiles are much less dependent on the CO_2 amount, although some cooling may still be observed, especially in the higher stratosphere where the temperature may be as low as 100 K.

5. A POSSIBLE EVOLUTIONARY SEQUENCE

In this section, a possible history of the surface temperature and the ozone abundance will be described. As mentioned above, Owen *et al.* (1979), Kasting *et al.* (1984) and Kiehl and Dickinson (1987) performed radiative–convective calculations to derive the time evolution of the mean surface temperature of the Earth resulting from the history of CO_2 and solar constant proposed by Hart (1978). These authors did not analyze the consequences of the variable amount of atmospheric ozone with time, and similarly they did not take the ice–albedo feedback into account. Here, both processes will be included in the model

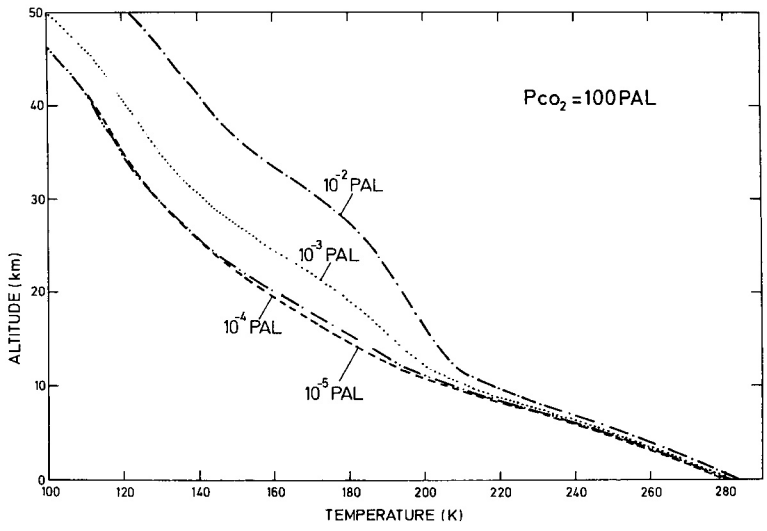

FIG. 12. VERTICAL TEMPERATURE PROFILES AT 100 PAL OF CO_2, FOR OXYGEN LEVELS VARYING FROM 10^{-5} TO 10^{-2} PAL.

and their contribution to the calculated temperature change will be estimated. A scenario for surface temperature and ozone will be calculated with the coupled model for 0.75, 2.0, 2.5 and 3.0 By BP, in addition to the $t = 0$ case corresponding to the standard model of Section 3.

The variation of the solar constant and the CO_2 pressure as a function of time are directly taken from Hart's scenario. For the oxygen level, the results of Hart's calculation were not adopted. For $t = 0.75$ By BP, the assumed oxygen level is 7×10^{-2} PAL. Indeed, this time period corresponds approximately to the first appearance of Metazoa ($\sim$670 By BP) and 7×10^{-2} PAL would be the lower limit of oxygen pressure allowing diffusion to a naked metazoan <1 mm thick (Cloud, 1983). This O_2 level is close to the value (8×10^{-2} PAL) calculated in Hart's scenario for the same epoch. The O_2 concentration in the atmosphere 2 By ago is not well-known. Cloud (1983) suggested a 1% O_2 level between 2.3 and 2.0 By BP. Besides, from the study of Precambrian paleosols and from the analysis of detrital uraninite survival in river sediments, Holland (1984) concluded that, between 2 and 3 By BP, the atmospheric oxygen pressure was comprised in the range of $10^{-2\,8}$ to 10^{-2} atm, that is 7.5×10^{-3}–5×10^{-2} PAL. In Hart's scenario, $f_{O_2} \simeq 5 \times 10^{-2}$ PAL, 2 By BP. It appears that all these studies propose an oxygen level between 1×10^{-2} and 5×10^{-2} PAL, 2 By BP. Here, a value of 2×10^{-2} PAL will be adopted. The O_2 levels 2.5 and 3 By BP are still much more poorly known and are equal to zero in Hart's scenario. According to Grandstaff (1980), the oxygen level would have been fluctuating between $\sim 10^{-6}$ and 10^{-2} PAL until the last important record of uraninites $\sim$2.3 By BP. In our time evolution, values of 10^{-3} and 10^{-4} PAL will be assumed for respectively 2.5 and 3 By BP. Note, however, that the value of the oxygen pressure 3 By ago is much debated and that, according to several workers, the atmosphere could have been much poorer in oxygen than assumed here, with ground level mixing ratios as low as 10^{-13}, as in the scenario proposed by Kasting (1987). Such low mixing ratios fall outside the range of O_2 levels considered here, so that we will not integrate this possibility into our calculation, although we do not exclude it. Nevertheless, the O_2 levels adopted in this section for the more recent past are in the range of permitted values shown in Fig. 6 of Kasting (1987).

The adopted surface pressure is obtained by adding the partial pressures of CO_2 and O_2 to the present N_2 amount. Thus, the presence of possibly large quantities of atmospheric methane is neglected and the surface pressure is not the same as in Hart's scenario.

The results of the radiative–convective and photochemical model for the above evolutionary sequence are presented in Table 2. It is seen that the partial pressure of CO_2 of Hart's scenario are large enough to compensate for the reduced solar luminosity, as evidenced by the works of Kiehl and Dickinson (1987) and Kasting *et al.* (1984). However, the surface temperature changes with respect to present conditions ΔT_s are smaller in these earlier studies than for the model of this paper. The larger ΔT_s calculated here are due to the additional effects that we considered

TABLE 2. A POSSIBLE HISTORY OF SURFACE TEMPERATURE AND OZONE

Time (By BP)	O_2 (PAL)	CO_2 (PAL)	Relative luminosity	P_s (atm)	T_s (K)	ΔT_s (K)	Ozone column (cm^{-2})
0.00	1	1.00	1.000	1.00	286.15	0.00	8.7×10^{18}
0.75	7×10^{-2}	1.00	0.958	0.81	280.45	−5.70	7.6×10^{18}
2.00	2×10^{-2}	26.88	0.889	0.80	283.88	−2.27	8.0×10^{18}
2.50	1×10^{-3}	56.25	0.861	0.81	281.16	−4.99	1.0×10^{18}
3.00	1×10^{-4}	103.13	0.833	0.83	280.21	−5.94	1.1×10^{17}

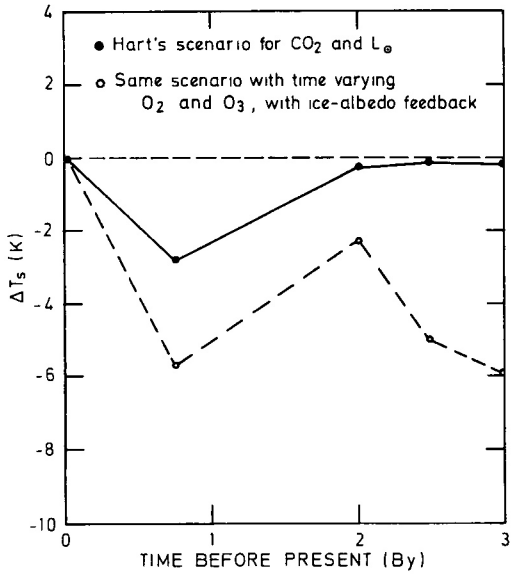

FIG. 13. TIME EVOLUTION OF THE SURFACE TEMPERATURE CALCULATED WITH THE EVOLUTIONARY SCENARIO OF THE SOLAR LUMINOSITY AND ATMOSPHERIC PRESSURES OF CO_2 AND O_2 PRESENTED IN TABLE 2.
The full line curve does not take the variations of O_2 and O_3 into account, while the dashed line does integrate them into the calculation.

simultaneously with the variations of the solar luminosity and the CO_2 partial pressure, that is the ice–albedo feedback and the changes in ozone and total pressure with time. To assess the importance of these additional effects in the climatic history of the Earth, the same calculation has been repeated without including the ice–albedo feedback and the variations of oxygen and ozone (that is with $P_0 = 1$ and a modern ozone profile). The results are displayed in Fig. 13 and compared with those listed in Table 2. The results for fixed ozone and oxygen have been obtained in the same conditions as assumed in the models of Kasting *et al.* (1984) and Kiehl and Dickinson (1987). They best compare with those of Kasting *et al.* (1984), due to the use of their parameterization for the CO_2 absorptances. Figure 13 shows that the inclusion of the variations in ozone, surface pressure and ground albedo is important and is far from generating a constant change in ΔT_s throughout the Earth's history. Further radiative–convective runs have been performed for $t = -3$ By to separate the contributions of these three factors to ΔT_s. As shown in Table 2, the complete model gives $\Delta T_s \simeq -5.94$ K for $t = -3$ By. If the ozone concentration is held fixed to the modern profile with $P_0 = 0.83$ atm, ΔT_s is only of −4.03 K. If both the ozone and the ground albedo are fixed, $\Delta T_s = -3.41$ K. Thus, the ice–albedo feedback amounts to only 0.62 K change in the surface temperature associated with the proposed evolutionary sequence. Finally, when the total pressure, the ground albedo and the ozone profile are not changed with respect to present conditions, the surface temperature drop is $\Delta T_s \simeq -0.10$ K. This last ΔT_s value is only due to the changes in CO_2 pressure and solar luminosity of Hart's evolutionary sequence. It is in reasonably good agreement with, although somewhat lower than, the −1.4 K value of Kasting *et al.* (1984) for the same epoch. Thus in summary, of the total temperature variation (with respect to present conditions) $\Delta T_s = -5.94$ K reported in Table 2 for $t = -3$ By, −1.91 K are due to the ozone decrease, −0.62 K to the change in surface albedo, −3.31 K to the reduction in total pressure and −0.10 K to the history of CO_2 and solar constant. Consequently, the global effect (−5.84 K) of the changes in ozone, surface albedo and total pressure is not negligible and should be taken into account in future studies of the Precambrian climate.

6. THE ULTRAVIOLET RADIATION FIELD AND ITS CONSEQUENCES FOR THE BIOSPHERE

During the early history of Earth, the larger amount of ultraviolet radiation reaching the surface may have been a serious cause of lethality in the primitive biosphere. In this section, we propose to analyze the effects on the Precambrian life of a deeper penetration of solar ultraviolet radiation into Earth's atmosphere. As above, the results will be presented as a function of the O_2 level.

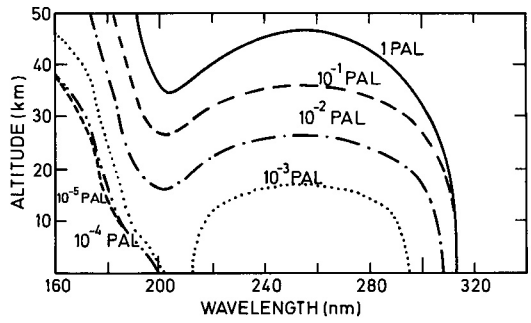

FIG. 14. ALTITUDE OF UNIT VERTICAL OPTICAL DEPTH IN THE ULTRAVIOLET.
The results are shown for atmospheres containing from 10^{-5} to 1 PAL of O_2 and 1 PAL of CO_2.

The first step in an analysis of the biological consequences of the reduced amounts of atmospheric oxygen and ozone consists in the calculation of the ultraviolet flux as a function of O_2. The second step is the decision of whether or not a given distribution of the ultraviolet radiation was tolerable for the primitive organisms. The calculation of the ultraviolet flux is implicitly contained in the model presented above. Figure 14 shows the altitude of the level where the radiative flux of a given wavelength is reduced to a fraction 1/e of its value at the top of the atmosphere. These curves were drawn for the model with 1 PAL of CO_2, they correspond to the total ozone column displayed in Fig. 1. As the O_2 level is decreased, the ozone peak is moved downward, so that the radiation penetrates deeper into the atmosphere. The absorption maximizes at $\sim$255 nm, whereas the penetration is easier for the radiation of the two spectral regions between $\sim$190 and 220 nm (where the absorption by O_2 is substantial) and above $\sim$300 nm. The radiation of these two regions is the first one to be a possible cause of lethality for the primitive organisms, when the atmospheric oxygen is decreased from the present level to 10^{-5} PAL. It is only when $f_{O_2} \leqslant 10^{-2}$ PAL that large amounts of ultraviolet radiation reach the troposphere. At 10^{-3} PAL, the radiation of the two regions mentioned above is very abundant in the troposphere and is still important at ground level. At 10^{-4} PAL, no ozone screen is present at all, since almost all the radiation with $\lambda > 200$ nm reaches the ground. The general shape of the curves displayed in Fig. 14 is similar to that derived by Blake and Carver (1977). However, at low levels of oxygen, these authors obtained a much larger ozone column than we do. Consequently, in our model, at 10^{-5}, 10^{-4} and 10^{-3} PAL the radiation penetrates deeper into the atmosphere.

In Fig. 15, the ultraviolet flux at ground level is displayed for various O_2 levels and is compared to the flux at the top of the atmosphere. These profiles can be thought of as representing the successive environmental conditions to which the Precambrian biosphere has been exposed. Similar results were obtained by Levine (1980), Levine *et al.* (1980) and Kasting (1987). The general agreement between our results and those of these studies is fairly good, although Kasting (1987) obtained a somewhat smaller penetration of the radiation of short wavelength (near $\sim$200 nm), due to the inclusion of the effects of Rayleigh scattering in his model. However, all the studies show that, as the level of oxygen is decreased, the surface ultraviolet flux with wavelengths between 195 and 230 nm or greater than 280 nm is the first to be increased. These wavelengths correspond to the two spectral regions mentioned while commenting on the results of Fig. 14. The window between 195 and 230 nm is located between the absorption of molecular oxygen and that of ozone. At large amounts of O_2, both oxygen and ozone contribute to close this window. An oxygen level as low as 10^{-4} PAL is necessary to allow the penetration to ground level of the radiation with wavelength between 230 and 280 nm. As we shall see later, this is precisely the domain in which the radiation is most efficient to create ultraviolet damages in living organisms. The problem which arises here is thus to determine to what degree the excess radiation in the two regions $\lambda > 280$ nm and $195 < \lambda < 230$ nm is lethal at 10^{-2} and 10^{-3} PAL.

The time when the primitive organisms were exposed to radiation with wavelengths between 230 and 280 nm appears to date back to a very remote past, since levels of oxygen lower than 10^{-3} PAL are required for this radiation to reach the surface. Possibly Archean life was already protected against this ultraviolet radiation soon after the appearance of greenplant photosynthesis (releasing oxygen). However, the exact dating of this event, as well as the atmospheric oxygen content more than 2 By BP are not well-known. The deposition of banded iron formations earlier than 3 By BP (Walker *et al.*, 1983) is not a proof of an important release of photosynthetic oxygen at that time, since abiotic photo-oxidation of hydrated Fe^{2+} can account for such a deposition (Braterman *et al.*, 1983; François, 1986, 1987). In addition, even if we assume that the banded iron formations are the products of iron oxidation by photosynthetic oxygen, their deposition did not require a high level of atmospheric oxygen (François and Gérard, 1986), in view of the presumably large concentration of Fe II in Archean oceanic basins.

In any case, however, it appears that an efficient

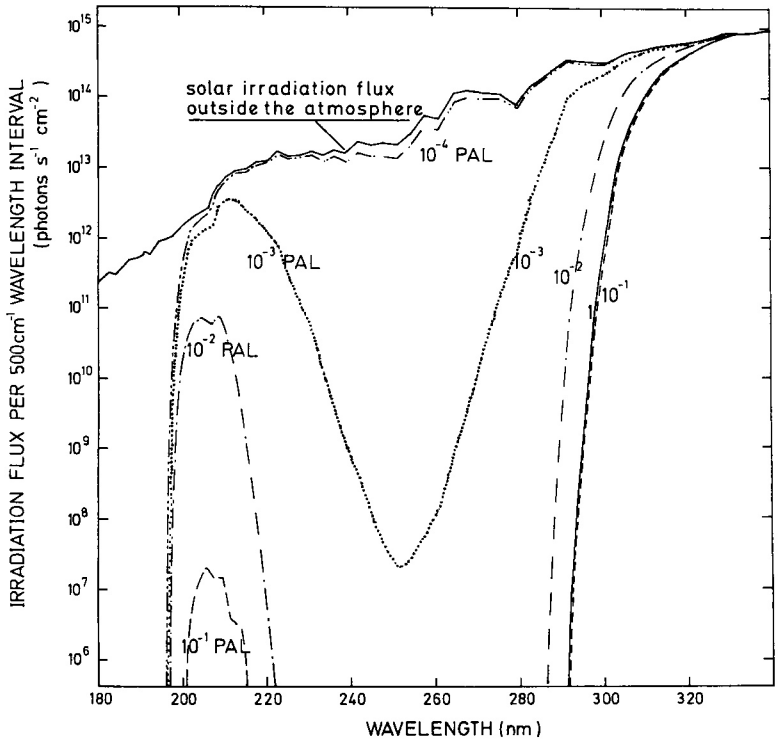

FIG. 15. WAVELENGTH DEPENDENCE OF THE SOLAR IRRADIATION FLUX AT GROUND LEVEL FOR ATMOSPHERIC OXYGEN LEVELS VARYING FROM 10^{-4} TO 1 PAL AND FOR 1 PAL OF CO_2.

ozone screen was established as early as 2 By BP, since, for an oxygen level between 10^{-2} and 5×10^{-2} PAL, the ozone column is larger than $\sim 50\%$ of its modern value. The irradiation curve for $t = -2$ By in our evolutionary scenario is displayed in Fig. 16. In this case, the ozone column is lower than at present by only 10%. The surface ultraviolet flux exhibits a small peak between 195 and 215 nm and a moderate increase above 290 nm. Presumably, this small change in the radiation field was of relatively minor environmental consequence. The situation was much different 2.5 By ago. At this time, the radiation flux was enhanced throughout the wavelength domain extending between ~ 195 and ~ 300 nm, showing just a sharp minimum near 251 nm, corresponding to the maximum in the ozone cross-section. Finally, 3.0 By ago, the flux above 195 nm at ground level was only slightly attentuated with respect to the solar flux outside the atmosphere. Presumably, the primitive organisms were able to support only very short exposure to such large ultraviolet fluxes.

It is not easy to decide whether a given dose of ultraviolet radiation was or was not lethal for the Precambrian biosphere. Indeed, early microorganisms protected themselves from lethal ultraviolet in several ways. The matting habit of blue–green algae, for instance, has been recognized as a protective mechanism against ultraviolet radiation (Monty, 1973; Margulis *et al.*, 1976). Negative phototaxis (swimming away from light) is also used by some prokaryotic organisms and the ability of repairing the ultraviolet damages either in the dark or by irradiation with visible light (photoreactivation) is well-known for bacteria, but is highly dependent on the species considered. Furthermore, some ultraviolet absorbers may have been present in the aquatic environment of primitive organisms. Liquid water itself absorbs weakly in the ultraviolet (Berkner and Marshall, 1965). Nitrite and nitrate (Rambler *et al.*, 1977), as well as many organic compounds (Sagan, 1973) can also offer a substantial protection.

In the present study, we do not integrate all these mechanisms in the model, since their contribution in protecting the Precambrian life is highly speculative. Rather, we calculate the fraction of inactivated microorganisms in a colony directly exposed to the ultra-

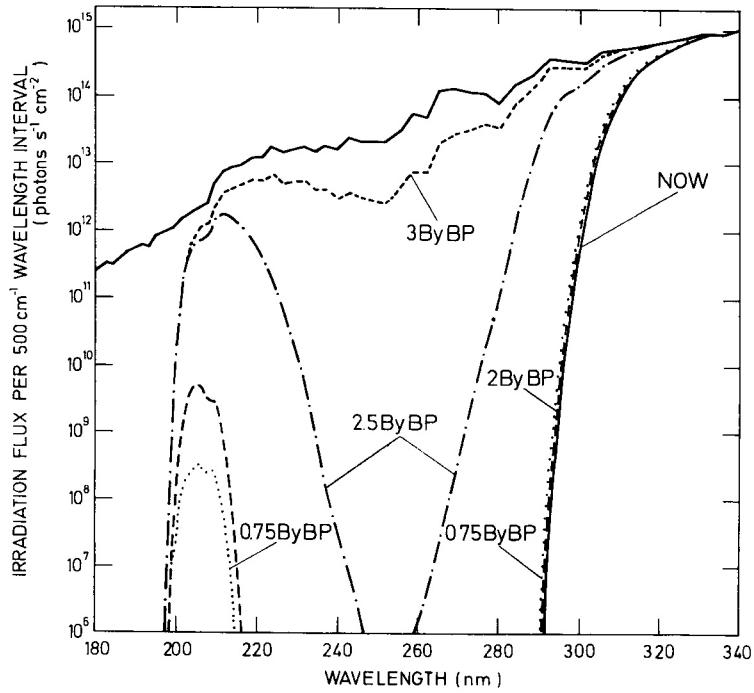

FIG. 16. WAVELENGTH DEPENDENCE OF THE SOLAR IRRADIATION FLUX AT GROUND LEVEL FOR THE EVOLUTIONARY SCENARIO OF TABLE 2.

violet fluxes presented above, that is, for an environment in which the only protection is the small amount of atmospheric ozone. The fraction of non inactivated bacteria (or surviving fraction) within a community irradiated with ultraviolet light is given by the survival curve, which depends on the wavelength λ and the bacterial species considered. This curve may be approximately fitted by the following expression

$$S = 1-(1-e^{-kF})^n \qquad (1)$$

where S is the surviving fraction, F is the fluence (or dose) of the ultraviolet radiation and n is the shoulder constant (Webb, 1977). The coefficient k is called the inactivation constant and corresponds to the slope of the surviving curve at high fluence. Rambler and Margulis (1980) have studied the resistance to ultraviolet irradiation of several bacteria under anaerobiosis. These authors give the survival curves of one obligate (*Clostridium sporogenes*) and several facultative (among which *Escherichia coli*) anaerobic bacteria irradiated with ultraviolet light of 254 nm. *Clostridium sporogenes* appears to be more resistant to irradiation than all the facultative anaerobes. Here, we use the survival curve of *Clostridium sporogenes* to estimate the resistance to ultraviolet of the primitive organisms. A comparison will be made with *Escherichia coli* whose resistance to irradiation is smaller. We shall also use the survival curve for the coccoid blue–green alga *Agmenellum quadruplicatum* from the measurements of Van Baalen and O'Donnell (1972). These survival curves enable the calculation of the inactivation constant k at 254 nm and the shoulder constant n. For *Clostridium sporogenes*, we find $k_{254} = 4.6 \times 10^{-17}$ cm^2 (per incident quantum) and $n \simeq 1.3$, for *Escherichia coli* $k_{254} = 2 \times 10^{-16}$ cm^2 and $n \simeq 4.3$ and for the blue–green alga *Agmenellum quadruplicatum*, $k_{254} = 5 \times 10^{-16}$ cm^2 and $n \simeq 38.3$. Consequently, this type of blue–green algae appears to be less resistant to ultraviolet radiation than the two bacteria considered (even *Escherichia coli*). However, it is not clear whether or not this conlusion is general for all types of blue–green algae (especially for the Precambrian ones), although in the experiments of Yopp *et al.* (1979), *Agmenellum quadruplicatum* is intermediate between *Anacystis nidulans* and *Aphanothece halophytica*, as far as the ultraviolet resistance is concerned.

The solar ultraviolet radiation is not monochromatic as the radiation used in the laboratory experiments. Therefore, to estimate the surviving fraction in a community of bacteria on the Precambrian Earth, relation (1) must be extended as follows

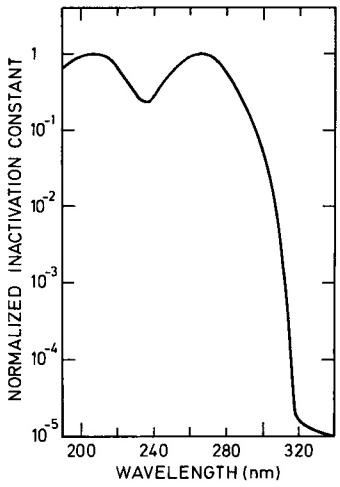

FIG. 17. WAVELENGTH DEPENDENCE OF NORMALIZED INACTIVATION CONSTANT k_λ USED IN THE CALCULATION OF THE SURVIVING FRACTION S IN A COLONY OF BACTERIA IRRADIATED WITH ULTRAVIOLET LIGHT.

$$S = 1-(1-e^{-\int k_\lambda dF_\lambda})^n \quad (2)$$

where dF_λ is the fluence in the wavelength internal $d\lambda$ used for the integration. In equation (2), it is assumed that the shoulder constant is independent of wavelength. Webb (1977) reports the wavelength dependence of k_λ for *Escherichia coli*. This action spectrum resembles that of thymidine absorptance between 240 and 313 nm, indicating that, in the ultraviolet, the lethality is caused by DNA damages. Consequently, the shape of the action spectrum should be relatively independent of the bacterial species. In what follows, this λ dependence will be adopted and extended to $\lambda < 240$ nm with the data of Voet *et al.* (1963) for the thymidine absorptance. The resulting action spectrum normalized to unity at its maximum value at ~ 267 nm is presented in Fig. 17. This action spectrum is used for *Clostridium sporogenes* and *Escherichia coli*. For *Agmanellum quadruplicatum*, the wavelength dependence of k_λ between 240 and 290 nm reported by Van Baalen and O'Donnell (1972) has been used, whereas, outside this interval, where the data are lacking, we have adopted the relative inactivation constant obtained above from the thymidine absorptance curve.

To calculate the fluence F_λ from the solar flux at the Earth's surface, we assume, following Ratner and Walker (1972), that the maximum irradiation time is ~ 4 h, corresponding to an exposure during the few hours of insolation around midday. This time is an upper limit, in view of the faster rotation rate of the Archean Earth (Walker *et al.*, 1983). The surviving fraction S calculated in these conditions for *Escherichia coli*, *Clostridium sporogenes* and *Agmenellum quadruplicatum*, under the various O_2 pressures considered in this paper, are presented in Table 3. For modern atmospheric conditions, $S = 0.61$ for *Escherichia coli*, 0.77 for *Clostridium sporogenes* and 0.48 for *Agmenellum quadruplicatum*, indicating that our criterion to estimate the surviving fraction is relatively strong. This small rate of lethality is due to the small amount of solar radiation between 305 and 310 nm reaching the ground for $f_{O_2} = 1$ PAL. The values of the surviving fraction given in Table 3 allow the comparison between the various models with different atmospheric O_2 contents. However, they do not measure the absolute rate of lethality, since the photoreactivation and dark repair mechansisms were probably efficient in the Archean biosphere. The importance of photoreactivation is well illustrated by the experiments of Rambler and Margulis (1980), in which a colony of Clostridia sporogenes inactivated to 99.9% was more than 80% photoreactivable. Here, we shall assume somewhat arbitrarily that the minimum value of S being tolerable in a colony of irradiated bacteria is 10^{-3}. We shall see later that the exact value of this minimum surviving rate is not really important, since the transition between high and negligible S values is very rapid, as O_2 and O_3 are removed from the atmosphere. From this criterion, it is clear that the ultraviolet threat should have been important only for $f_{O_2} \leqslant 10^{-3}$ PAL, except for the blue–green alga *Agmenellum quadruplicatum*, for which an O_2 level of 10^{-2} PAL is already critical. The surviving fraction after a 4 h exposure time was also calculated for the evolutionary scenario proposed in Section 5. These results are also lited in Table 3. The rate of lethality would have been important 2.5 and 3.0 By ago even for *Clostridium sporogenes*, in spite of the larger CO_2 amount at these times.

The same method was used to calculate the values of S as a function of the total ozone column. The results are presented in Fig. 18 for the two bacteria and the blue–green alga considered above. In this calculation, it was assumed that ozone was the only absorbing species in the ultraviolet region considered and, thus, possible absorption by O_2 and CO_2 for the shortest wavelengths is neglected. From these curves, it may be seen that the drop in the values of S with decreasing ozone is very sharp, so that the ozone column interval in which S goes to zero is relatively narrow. This observation allows us to define with a rather good accuracy a minimum ozone column being tolerable by the organisms considered, when no additional protecting mechanism is present. If, as above, we assume that the minimum acceptable value of S is 10^{-3}, we obtain minimum ozone columns of

TABLE 3. SURVIVING FRACTION FOR TWO TYPES OF BACTERIA (*Escherichia coli* AND *Clostridium sporogenes*) AND FOR THE BLUE–GREEN ALGA *Agmenellum quadruplicatum* AFTER A 4 h EXPOSURE TO THE ULTRAVIOLET RADIATION REACHING THE GROUND FOR ATMOSPHERIC LEVELS OF OXYGEN VARYING FROM 10^{-5} TO 1 PAL. The results are also given for the evolutionary sequence described in Section 5

Time (By BP)	CO_2 level (PAL)	O_2 level (PAL)	Surviving fraction *Escherichia coli*	*Clostridium sporogenes*	*Agmenellum quadruplicatum*
	1	1	0.74	0.77	0.48
	1	10^{-1}	0.80	0.78	0.54
	1	10^{-2}	0.24	0.35	5.2×10^{-4}
	1	10^{-3}	0	1.5×10^{-9}	0
	1	10^{-4}	0	0	0
	1	10^{-5}	0	0	0
0.75	1	7×10^{-2}	0.40	0.69	0.15
2.00	26	2×10^{-2}	0.48	0.72	0.25
2.50	56	10^{-3}	0	1.8×10^{-6}	0
3.00	103	10^{-4}	0	0	0

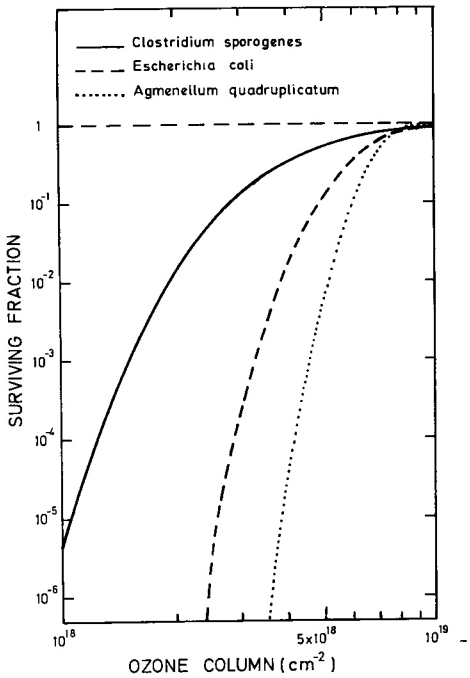

FIG. 18. CALCULATED SURVIVING FRACTIONS IN VARIOUS BACTERIAL OR CYANOBACTERIAL COLONIES AFTER A 4 h IRRADIATION TIME WITH SOLAR ULTRAVIOLET RADIATION ATTENUATED BY A SPECIFIED OZONE AMOUNT.

approximately 1.5×10^{18}, 3.3×10^{18} and 4.5×10^{18} cm^{-2}, being tolerable by respectively, *Clostridium sporogenes*, *Escherichia coli* and *Agmenellum quadruplicatum*. These values are all substantially lower than those estimated previously by Berkner and Marshall (1965) (5.6×10^{18} cm^{-2}) and Ratner and Walker (1972) (7×10^{18} cm^{-2}) for the minimum ozone column required to produce a full ultraviolet screen. For *Agmenellum quadruplicatum*, the minimum ozone column calculated here is only slightly smaller than the presently observed column in the spring time ozone hole of Antarctica, pointing out the possible extreme fragility of these living organisms. However, the Precambrian blue–green algae presumably developed capabilities of matting to protect themselves against lethal ultraviolet. In these conditions, the minimum ozone column being tolerable by these organisms would have been much lower and possibly, as proposed by Rambler and Margulis (1980), the simultaneous use of all additional protective mechanisms, coupled to the frequent opportunities for dark ultraviolet repair, would have allowed the development and the persistence of the Archean life, despite the intense ultraviolet flux at that time. Nevertheless, from our calculation, we may conclude that an ultraviolet screen strong enough to enable an unprotected bacterial life during the Precambrian would have been established as soon as the ozone column has exceeded $\sim2\times10^{18}$ to $\sim4\times10^{18}$ cm^{-2}, that is when the oxygen level has become larger than several times 10^{-3} PAL.

In Fig. 19, the wavelength distribution of the effects of the ultraviolet radiation on *Clostridium sporogenes* is shown for f_{O_2} varying from 10^{-5} to 10^{-2} PAL. The quantity displayed is $\exp(-k_\lambda\, dF_\lambda)$ where dF_λ is the fluence in a 500 cm^{-1} interval around wavelength λ. Both ultraviolet windows mentioned above (195 nm $< \lambda <$ 230 nm and $\lambda >$ 280 nm) contribute to the increased lethality as the atmospheric oxygen level is decreased. However, the efficiency is larger for $\lambda >$ 280 nm. This radiation is thus the main contributor to the decrease in the surviving fraction and the other atmospheric window (195 $< \lambda <$ 230 nm) appears to play a secondary role. This result *a pos-*

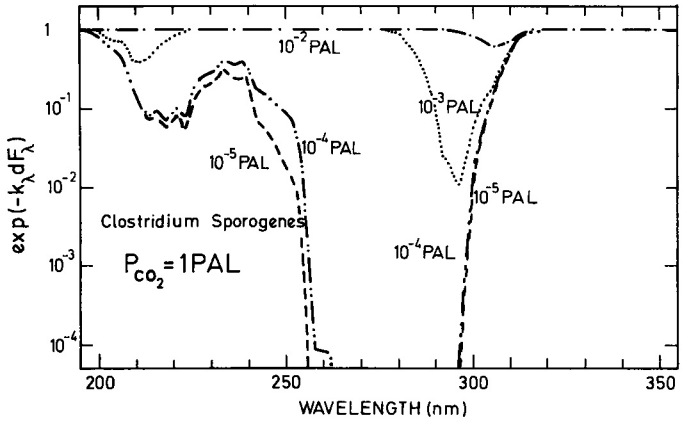

FIG. 19. CONTRIBUTION OF EACH ULTRAVIOLET WAVELENGTH λ TO THE RATE OF LETHALITY OF *Clostridium sporogenes* AT SEVERAL OXYGEN LEVELS.
The quantity displayed is the factor $\exp(-k_\lambda dF_\lambda)$ where dF_λ is the fluence in a 500 cm^{-1} interval around λ and k_λ is the inactivation constant at this wavelength.

teriori justifies our neglect of Rayleigh scattering in the photochemical scheme, since this process mainly affects the intensity of the radiation in the 195–230 nm atmospheric window.

7. CONCLUSIONS

In this paper, we have analyzed the effects of the lower oxygen level on the climatology, the ozone content and the ultraviolet radiation at ground level on the Precambrian Earth. The climatic consequences of a lower ozone content in the past are important, since removing O_2 and O_3 from the modern atmosphere would produce a temperature decrease of $\sim$7.2 K. The stratospheric thermal structure would be changed progressively as the oxygen level is decreased from 1 to 10^{-5} PAL, the stratospheric maximum disappearing approximately at 10^{-2} PAL.

Enhancing the CO_2 level from 1 to 100 PAL substantially increases the ozone column at 10^{-5} and 10^{-4} PAL of O_2, but does not change it importantly at higher O_2 levels. Furthermore, the stratospheric temperature is slightly decreased with respect to the model with 1 PAL of CO_2.

An evolutionary scenario for the global mean surface temperature based on the CO_2 history calculated by Hart (1978) and on a likely time variation of O_2 has been proposed for the last 3 By. This scenario differs substantially from calculations made in previous studies, showing the important climatic role of the time evolution of O_2 and O_3.

The flux of ultraviolet radiation at ground level has been calculated as a function of wavelength for all the models considered in this study and the implications for the Precambrian biosphere have been examined. The rate of lethality in bacterial colonies should be important only for oxygen levels somewhat lower than $\sim 10^{-2}$ PAL, that is more than $\sim$2 By ago. At this time, the atmospheric CO_2 level was much larger than today and may have contributed to slightly enhance the ozone column, reducing the ultraviolet radiation at ground level between $\sim$220 and $\sim$280 nm. However, the irradiation flux was not small enough to preserve the primitive biosphere from a high rate of lethality at O_2 levels lower than 10^{-3} PAL, even if a large amount of atmospheric CO_2 is assumed. Very early in Earth's history, the CO_2 level was probably much larger than the values considered here, but at this time photosynthesis was not active yet, so that the oxygen level and the ozone column were probably low. Nevertheless, if between $\sim$ 3 and 2 By ago the CO_2 content was larger than in Hart's scenario, a more efficient shielding from solar ultraviolet would have existed at this time, reducing the lethality of the microorganisms. A definitive conclusion about this CO_2 effect must await more geological evidences or reliable geochemical models are available for the Archean period.

Nevertheless, independently of this evolutionary problem, we have shown that an ozone screen adequate to enable the existence of unprotected bacterial life would have been established, as soon as the total column of atmospheric ozone has exceeded $\sim 2 \times 10^{18}$–$\sim 4 \times 10^{18}$ cm^{-2}, depending on the bacterial species considered, a value which is substantially less than the previous estimates by Berkner and Marshall (1965) and Ratner and Walker (1972).

Acknowledgements—One of us (J.C.G.) is supported by the Belgian Fund for Scientific Research. Financial assistance of this research by grants FNRS 1.5.223.88 F and 1.5.710.87 F is gratefully acknowledged.

REFERENCES

Baulch, D. L., Drysdale, D. D., Duxbury, J. and Grant, S. J. (1976) *Evaluated kinetic data for high temperature reactions—3. Homogeneous gas phase reactions of the O_2–O_3 system, the CO–O_2–H_2 system, and of the sulfur-containing species.* Butterworth, Woburn, Massachusetts.

Bell, J. A. (1971) Methylene reaction rates, quantum yields in the diazomethane–propane photolysis system: effects of photolysis time, reactant ratios, and added gases. *J. phys. Chem.* **75**, 1537.

Berkner, L. V. and Marshall, L. C. (1965) On the origin and rise of oxygen concentration in the Earth's atmosphere. *J. atmos. Sci.* **22**, 225.

Blake, A. J. and Carver, H. J. (1977) The evolutionary role of atmospheric ozone. *J. atmos. Sci.* **34**, 720.

Brasseur, G. and Simon, P. C. (1981) Stratospheric chemical and thermal response to long-term variability in solar u.v. irradiance. *J. geophys. Res.* **86**, 7343.

Brasseur, G. and Solomon, S. (1984) *Aeronomy of the Middle Atmosphere.* Reidel, Dordrecht.

Braterman, P. S., Cairns-Smith, A. G. and Sloper, R. W. (1983) Photo-oxidation of hydrated Fe^{2+}-significance for banded iron formations. *Nature* **303**, 163.

Braun, W., Bass, A. M. and Pilling, M. (1970) Flash photolysis of ketene and diazomethane: the production and reaction kinetics of triplet and singlet methylene. *J. chem. Phys.* **52**, 5131.

Burch, D. E., Gryvnak, D., Singleton, E. B., France, W. L. and Williams, D. (1962) Infrared absorption by carbon dioxide, water vapor, and minor atmospheric constituents. AFCRL-62-698.

Campbell, J. M. and Trush, B. A. (1967) The association of oxygen atoms and their combination with nitrogen atoms. *Proc. R. Soc. (London) Ser A* **296**, 222.

Cheng, J. T. and Yeh, C. (1977) Pressure dependence of the rate constant of the reaction $H+CH_3 \rightarrow CH_4$. *J. phys. Chem.* **81**, 1982.

Cloud, P. (1983) Aspects of Proterozoic biogeology. *Geol. Soc. Am. Mem.* **161**, 245.

Clyne, M. and Monkhouse, P. (1977) Atomic resonance fluorescence for rate constants of rapid biomolecular reactions—5. Hydrogen atoms reactions; $H+NO_2$ and $H+O_3$. *J. chem. Soc. Faraday Trans.* 2 **73**, 298.

Donner, L. and Ramanathan, V. (1980) Methane and nitrous oxide: their effects on the terrestrial climate. *J. atmos. Sci.* **37**, 119.

Endal, A. S. and Schatten, K. H. (1982) The faint young sun-climate paradox: continental influences. *J. geophys. Res.* **87**, 7295.

Fishman, J. and Crutzen, P. J. (1977) A numerical study of tropospheric photochemistry using a one-dimensional model. *J. geophys. Res.* **82**, 5897.

François, L. M. (1986) Extensive deposition of banded iron formations was possible without photosynthesis. *Nature* **320**, 352.

François, L. M. (1987) Reducing power of ferrous iron in the Archean ocean, role of $FeOH^+$ photooxidation. *Paleoceanography* **2**, 395.

François, L. M. (1988) The effect of cloud parameterization and temperature profile on the climate sensitivity to ozone perturbations. *Atmos. Res.* **21**, 305.

François, L. M. and Gérard, J. C. (1986) Reducing power of ferrous iron in the Archean ocean—1. Contribution of photosynthetic oxygen. *Paleoceanography* **1**, 355.

Gérard, J.-C. and François, L. M. (1987) A model of solar-cycle effects on palaeoclimate and its implications for the Elatina Formation. *Nature* **326**, 577.

Gérard, J.-C. and François, L. M. (1988) A sensitivity study of the effects of solar luminosity changes on the Earth's global temperature. *Ann. Geophys.* **6**, 101.

Grandstaff, D. E. (1980) Origin of uraniferous conglomerates at Elliott Lake, Canada, and Witwatersrand, South Africa: implication for oxygen in the Precambrian atmosphere. *Precambrian Res.* **13**, 1.

Hampson, R. F. and Garvin, D. (1977) Reaction rate and photochemical data for atmospheric chemistry—1977. *NBS Spec. Publ. U.S.* **513**.

Hart, M. H. (1978) The evolution of the atmosphere of the Earth. *Icarus* **33**, 23.

Hesstvedt, E., Henriksen, S. E. and Hjartarson, H. (1974) On the development of an anaerobic atmosphere, a model experiment. *Geophys. norvegica* **31**, 1.

Hochanadel, C. J., Sworski, T. J. and Ogren, P. J. (1980) Ultraviolet spectrum and reaction kinetics of the formyl radical. *J. phys. Chem.* **84**, 231.

Holland, H. D. (1984) *The Chemical Evolution of the Atmosphere and Oceans.* Princeton University Press, Princeton.

Hunten, D. M. (1975) Vertical transport in atmospheres, in *Earth and Planets* (Edited by McCormac, B. M.). D. Reidel, Higham, Massachusetts.

Inn, E. C. Y., Watanabe, K. and Zelikoff, M. (1953) Absorption coefficients of gases in the vacuum ultraviolet—3. CO_2. *J. chem. Phys.* **21**, 1648.

Iribarne, J. V. and Godson, W. L. (1981) *Atmospheric Thermodynamics* (Second Edition). D. Reidel, Dordrecht.

Jet Propulsion Laboratory (1983) Chemical kinetic and photochemical data for use in stratospheric modeling. *JPL Publ. 83–62*, Jet. Propul. Lab., Pasadena, California.

Jet Propulsion Laboratory (1985) Chemical kinetic and photochemical data for use in stratospheric modeling. *JPL Publ. 85–37*, Jet Propul. Lab., Pasadena, California.

Johnston, H. S. and Selwyn, G. (1975) New cross-sections of the absorption of near ultraviolet radiation by nitrous oxide (N_2O). *Geophys. Res. Lett.* **2**, 549.

Kasting, J. F. (1979) Evolution of oxygen and ozone in the Earth's atmosphere. Ph.D. Dissertation, University of Michigan, Ann Arbor.

Kasting, J. F. (1985) Photochemical consequences of enhanced CO_2 levels in Earth's early atmosphere, *The carbon cycle and atmospheric CO_2: natural variations Archean to present* (Edited by Sundquist, E. T. and Broecher, W. S.). *Geophysical Monograph* **32**. American Geophysical Union, Washington, D.C.

Kasting, J. F. (1987) Theoretical constraints on oxygen and carbon dioxide concentrations in the Precambrian atmosphere. *Precambrian Res.* **34**, 205.

Kasting, J. F. and Donahue, T. M. (1980) The evolution of atmospheric ozone. *J. geophys. Res.* **85**, 3255.

Kasting, J. F., Holland, H. D. and Pinto, J. P. (1985) Oxidant abundances in rainwater and the evolution of atmospheric oxygen. *J. geophys. Res.* **90**, 10497.

Kasting, J. F., Pollack, J. B. and Crisp, D. (1984) Effects of

high CO_2 levels on surface temperature and atmospheric oxidation state of the early Earth. *J. atmos. Chem.* **1**, 403.
Kiehl, J. T. and Dickinson, R. E. (1987) A study of the radiative effects of enhanced atmospheric CO_2 and CH_4 on early Earth surface temperatures. *J. geophys. Res.* **92**, 2991.
Lacis, A. A. and Hansen, J. E. (1974) A parameterization for the absorption of solar radiation in the Earth's atmosphere. *J. atmos. Sci.* **31**, 118.
Laufer, A. H. and Bass, A. M. (1974) Rate constants for reactions of methylene with carbon monoxide, oxygen, nitric oxide, and acetylene. *J. phys. Chem.* **78**, 1344.
Levine, J. S. (1980) Surface ultraviolet radiation for paleoatmospheric levels of oxygen and ozone. *Origins of Life* **10**, 313.
Levine, J. S. and Boughner, R. E. (1979) The effect of paleoatmospheric ozone on surface temperature. *Icarus* **39**, 310.
Levine, J. S., Augustsson, T. R., Boughner, R. E., Natarajan, M. and Sacks, L. J. (1981) Comets and the photochemistry of the paleoatmosphere, in *Comets and the Origins of Life* (Edited by Ponnamperuma, C.). D. Reidel, Dordrecht.
Levine, J. S., Boughner, R. E. and Smith, K. A. (1980) Ozone, ultraviolet flux and temperature of the plaeoatmosphere. *Origins of Life* **10**, 199.
Levine, J. S., Hays, P. B. and Walker, J. C. G. (1979) The evolution and variability of atmospheric ozone over geological time. *Icarus* **39**, 295.
Lindzen, R. S., Hou, A. Y. and Farrell, B. F. (1982) The role of convective model choice in calculating the climate impact of doubling CO_2. *J. atmos. Sci.* **39**, 1189.
Liu, S. C. and Donahue, T. M. (1974) Realistic model of hydrogen constituents in the lower atmosphere and escape flux from the upper atmosphere. *J. atmos. Sci.* **31**, 2238.
Manabe, S. and Wetherald, R. T. (1967) Thermal equilibrium of the atmosphere with a given distribution of relative humidity. *J. atmos. Sci.* **24**, 241.
Margulis, L., Walker, J. C. G. and Rambler, M. (1976) Reassessment of roles of oxygen and ultraviolet light in Precambrian evolution. *Nature* **264**, 620.
McEwan, M. J. and Phillips, L. F. (1975) *Chemistry of the Atmosphere*. Wiley, New York.
Monty, C. V. (1973) Les nodules de manganèse sont des stromatolithes océaniques. *C. r. Acad. Sci. Paris* **276**, 3285.
Morss, D. A. and Kuhn, W. R. (1978) Paleoatmospheric temperature structure. *Icarus* **33**, 40.
Mount, G. H., Warden, E. S. and Moos, H. W. (1977) Photoabsorption cross-sections of methane from 1400 to 1850 Å. *Astrophys. J.* **214**, L47.
Nicoli, M. P. and Visconti, G. (1982) Impact of coupled perturbations of atmospheric gases on Earth's climate and ozone. *Pageoph.* **120**, 626.
Owen, T., Cess, R. D. and Ramanathan, V. (1979) Enhanced CO_2 greenhouse to compensate for reduced solar luminosity on early Earth. *Nature* **277**, 640.
Pinto, J. P., Gladstone, C. R. and Yung, Y. L. (1980) Photochemical production of formaldehyde in Earth's primitive atmosphere. *Science* **210**, 183.
Ramanathan, V. (1976) Radiative transfer within the Earth's troposphere and stratosphere: a simplified radiative-convective model. *J. atmos. Sci.* **33**, 1330.
Ramanathan, V. and Dickinson, R. E. (1979) The role of stratospheric ozone in the zonal and seasonal radiative energy balance of the Earth–troposphere system. *J. atmos. Sci.* **36**, 1084.
Ramanathan, V., Pitcher, E. J., Malone, R. C. and Blackmon, M. L. (1983) The response of spectral general circulation model to refinements in radiative processes. *J. atmos. Sci.* **40**, 605.
Rambler, M. B. and Margulis, L. (1980) Bacterial resistance to ultraviolet irradiation under anaerobiosis: implications for pre-Phanerozoic evolution. *Science* **210**, 638.
Rambler, M. B., Margulis, L. and Barghoorn, E. S. (1977) *Chemical Evolution and the Precambrian* (Edited by Ponnamperuma, C.), p. 133. Academic Press, New York.
Ratner, M. I. and Walker, J. C. G. (1972) Atmospheric ozone and the history of life. *J. atmos. Sci.* **29**, 803.
Sagan, C. (1973) Ultraviolet selection pressure on the earliest organisms. *J. theo. Biol.* **39**, 195.
Sagan, C. and Mullen, G. (1972) Earth and Mars: evolution of atmospheres and surface temperatures. *Science* **177**, 52.
Sasamori, T. (1968) The radiative cooling calculation for application to general circulation experiments. *J. appl. Meteorol.* **7**, 721.
Selwyn, G., Podolske, J. and Johnston, H. S. (1977) Nitrous oxide ultraviolet absorption spectrum at stratospheric temperatures. *Geophys. Res. Lett.* **4**, 427.
Shemansky, D. E. (1972) CO_2 extinction coefficient 1700–3000 Å. *J. chem. Phys.* **56**, 1582.
Sworski, T. J., Hochanadel, C. J. and Ogren, P. J. (1980) Flash photolysis of H_2O vapor in CH_4. *J. phys. Chem.* **84**, 129.
Thompson, B. A., Harteck, P. and Reeves, R. R. (1963) Ultraviolet absorption coefficients of CO_2, CO, O_2, H_2O, N_2O, NH_3, NO, SO_2 and CH_4 between 1850 and 4000 Å. *J. geophys. Res.* **68**, 6431.
Van Baalen, C. and O'Donnell, R. (1972) Action spectra for ultraviolet killing and photoreactivation in the blue–green alga *Agmenellum quadruplicatum*. *Photochem. Photobiol.* **15**, 269.
Visconti, G. (1982) Radiative–photochemical models of the primitive terrestrial atmosphere. *Planet. Space Sci.* **30**, 785.
Voet, D., Gratzer, W. B., Cox, R. A. and Doty, P. (1963) Absorption spectra of nucleotides, polynucleotides, and nucleic acids in the far ultraviolet. *Biopolymers* **1**, 193.
Walker, J. C. G. (1977) *Evolution of the Atmosphere*. Macmillan, New York.
Walker, J. C. G., Hays, P. B. and Kasting, J. F. (1981) A negative feedback mechanism for the long-term stabilization of Earth's surface temperature. *J. geophys. Res.* **86**, 9776.
Walker, J. C. G., Klein, C., Schidlowski, M., Schopf, J. W., Stevenson, D. J. and Walter, M. R. (1983) Environmental evolution of the Archean-early Protozoic Earth, in *Earth's Earliest Biosphere: its Origin and Evolution* (Edited by Schopf, J. W.). Princeton University Press, Princeton.
Wang, W. C., Pinto, J. P. and Yung, Y. L. (1980) Climatic effects due to halogenated components in the Earth's atmosphere. *J. atmos. Sci.* **37**, 333.
Wang, W. C. and Stone, P. H. (1980) Effect of ice–albedo feedback on global sensitivity in a one-dimensional radiative–convective climate model. *J. atmos. Sci.* **37**, 545.
Watanabe, K., Zelikoff, M. and Inn, E. C. Y. (1953) Absorption coefficients of oxygen in the vacuum ultraviolet. *J. chem. Phys.* **21**, 1026.
Webb, R. B. (1977) Lethal and mutagenic effects of near-ultraviolet radiation, in *Photochemical and Photobiological*

Reviews, Vol. 2 (Edited by Smith, K. C.). Plenum Press, New York.
Williams, G. E. and Sonnet, C. P. (1985) Solar signature in sedimentary cycles from the late Precambrian Elatina formation, Australia. *Nature* **318**, 523.
Yopp, J. H., Albright, G. and Miller, D. M. (1979) Effects of antibiotics and ultraviolet radiation on the halophylic blue–green alga, *Aphanothece halophytica*. *Botanica Marina* **22**, 167.
Zelikoff, M., Watanabe, K. and Inn, E. C. Y. (1953) Absorption coefficient of gases in the vacuum ultraviolet—2. Nitrous oxide. *J. chem. Phys.* **21**, 1643.